Behavioral/Cognitive

Enhanced Retrieval of Taste Associative Memory by Chemogenetic Activation of Locus Coeruleus Norepinephrine Neurons

Ryoji Fukabori,[1*] Yoshio Iguchi,[1*] Shigeki Kato,[1] Kazumi Takahashi,[2] Satoshi Eifuku,[2] Shingo Tsuji,[3] Akihiro Hazama,[3] Motokazu Uchigashima,[4] Masahiko Watanabe,[4] Hiroshi Mizuma,[5] Yilong Cui,[6] Hirotaka Onoe,[7] Keigo Hikishima,[8] Yasunobu Yasoshima,[9] Makoto Osanai,[10] Ryo Inagaki,[10] Kohji Fukunaga,[11] Takuma Nishijo,[12] Toshihiko Momiyama,[12] Richard Benton,[13] and Kazuto Kobayashi[1]

[1]Department of Molecular Genetics, Institute of Biomedical Sciences, Fukushima Medical University School of Medicine, Fukushima 960-1295, Japan, [2]Department of Systems Neuroscience, Fukushima Medical University School of Medicine, Fukushima 960-1295, Japan, [3]Department of Cellular and Integrative Physiology, Fukushima Medical University School of Medicine, Fukushima 960-1295, Japan, [4]Department of Anatomy, Faculty of Medicine, Hokkaido University, Sapporo 060-8638, Japan, [5]Laboratory for Pathophysiological and Health Science, RIKEN Center for Biosystems Dynamics Research, Kobe 650-0047, Japan, [6]Laboratory for Biofunction Dynamics Imaging, RIKEN Center for Biosystems Dynamics Research, Kobe 650-0047, Japan, [7]Human Brain Research Center, Kyoto University Graduate School of Medicine, Kyoto 606-8501, Japan, [8]Medical Devices Research Group, Health and Medical Research Institute, National Institute of Advanced Industrial Science and Technology (AIST), Tsukuba 305-8564, Japan, [9]Division of Behavioral Physiology, Department of Behavioral Sciences, Graduate School of Human Science, Osaka University, Suita 565-0871, Japan, [10]Department of Radiological Imaging and Informatics, Graduate School of Medicine, Tohoku University, Sendai 980-8575, Japan, [11]Department of Pharmacology, Graduate School of Pharmaceutical Sciences, Tohoku University, Sendai 980-8575, Japan, [12]Department of Pharmacology, Jikei University School of Medicine, Tokyo 105-8461, Japan, and [13]Center for Integrative Genomics, Faculty of Biology and Medicine, University of Lausanne, CH-1015 Lausanne, Switzerland

The ability of animals to retrieve memories stored in response to the environment is essential for behavioral adaptation. Norepinephrine (NE)-containing neurons in the brain play a key role in the modulation of synaptic plasticity underlying various processes of memory formation. However, the role of the central NE system in memory retrieval remains unclear. Here, we developed a novel chemogenetic activation strategy exploiting insect olfactory ionotropic receptors (IRs), termed "IR-mediated neuronal activation," and used it for selective stimulation of NE neurons in the locus coeruleus (LC). *Drosophila melanogaster* IR84a and IR8a subunits were expressed in LC NE neurons in transgenic mice. Application of phenylacetic acid (a specific ligand for the IR84a/IR8a complex) at appropriate doses induced excitatory responses of NE neurons expressing the receptors in both slice preparations and *in vivo* electrophysiological conditions, resulting in a marked increase of NE release in the LC nerve terminal regions (male and female). Ligand-induced activation of LC NE neurons enhanced the retrieval process of conditioned taste aversion without affecting taste sensitivity, general arousal state, and locomotor activity. This enhancing effect on taste memory retrieval was mediated, in part, through α_1- and β-adrenergic receptors in the basolateral nucleus of the amygdala (BLA; male). Pharmacological inhibition of LC NE neurons confirmed the facilitative role of these neurons in memory retrieval via adrenergic receptors in the BLA (male). Our findings indicate that the LC NE system, through projections to the BLA, controls the retrieval process of taste associative memory.

Key words: **basolateral amygdala; chemogenetic tool; conditioned taste aversion; ionotropic receptor; locus coeruleus; memory retrieval**

Received July 4, 2020; revised Aug. 28, 2020; accepted Sep. 21, 2020.

Author contributions: R.F., Y.I., R.B., and K.K. designed research; R.F., Y.I., S.K., K.T., S.T., A.H., M.U., M.W., M.O., R.I., T.N., and T.M. performed research; S.K., M.U., M.W., H.M., Y.C., H.O., K.H., Y.Y., K.F., R.B., and K.K. contributed unpublished reagents/analytic tools; R.F., Y.I., K.T., S.E., S.T., A.H., M.U., M.W., M.O., R.I., T.N., and T.M. analyzed data; R.F., Y.I., S.K., K.T., H.M., Y.C., H.O., M.O., T.M., R.B., and K.K. wrote the paper.

This work was supported by grants-in-aid for Scientific Research on Innovative Areas Adaptive Circuit Shift (Grant 26112002) from the Ministry of Education, Science, Sports, and Culture of Japan, and Core Research for Evolutional Science and Technology (Grant JP16gm0310008) of Japan Science and Technology Agency (K.K.); and by a European Research Council Consolidator Grant (Grant 615094), a Human Frontier Science Program Young Investigator Award (Grant RGY0073/2011), and the Swiss National Science Foundation Nano-Tera Envirobot Project (20NA21_143082; R.B.). We thank Minako Kikuchi, Noriko Sato, Hiromi Hashimoto, and Masateru Sugawara (Fukushima Medical University) for technical support during animal experiments; and Tomoko Kobayashi (Fukushima Medical University) for helpful illustrations.

The authors declare no competing financial interests.

*R.F. and Y.I. contributed equally to this work.

M. Uchigashima's present address: Research Center for Pharmaceutical Development, Graduate School of Pharmaceutical Sciences, Tohoku University, Sendai 980-8579, Japan.

M. Osanai's present address: Department of Medical Physics and Engineering, Division of Health Sciences, Osaka University Graduate School of Medicine, Suita 565-0871, Japan.

R. Inagaki's present address: Research Center for Pharmaceutical Development, Graduate School of Pharmaceutical Sciences, Tohoku University, Sendai 980-8579, Japan.

T. Nishijo's present address: Department of Molecular Neurobiology, Institute for Developmental Research, Aichi Developmental Disability Center, Kasugai 480-0392, Japan.

Correspondence should be addressed to Kazuto Kobayashi at kazuto@fmu.ac.jp.

https://doi.org/10.1523/JNEUROSCI.1720-20.2020

Significance Statement

Norepinephrine (NE)-containing neurons in the brain play a key role in the modulation of synaptic plasticity underlying various processes of memory formation, but the role of the NE system in memory retrieval remains unclear. We developed a chemogenetic activation system based on insect olfactory ionotropic receptors and used it for selective stimulation of NE neurons in the locus coeruleus (LC) in transgenic mice. Ligand-induced activation of LC NE neurons enhanced the retrieval of conditioned taste aversion, which was mediated, in part, through adrenoceptors in the basolateral amygdala. Pharmacological blockade of LC activity confirmed the facilitative role of these neurons in memory retrieval. Our findings indicate that the LC–amygdala pathway plays an important role in the recall of taste associative memory.

Introduction

The ability to retrieve necessary information associated with environmental stimuli and context is indispensable for animal behavioral adaptation. Disturbances in this information retrieval process, especially in humans, result in degradation of not only quality of life but also the sense of personal identity (Klein and Nichols, 2012). Impairments specific to the retrieval process have been reported in some amnesiac patients, who exhibit the inability to explicitly recall test stimuli despite their spared implicit memory of the same stimuli, which can be retrieved with prompts or partial information (Warrington and Weiskrantz, 1970). By contrast, recurrent involuntary memory retrieval after traumatic events is one of the major symptoms of post-traumatic stress disorder (American Psychiatric Association, 2013). A number of clinical and preclinical studies have suggested that multiple neurotransmitter/modulator systems are implicated in the retrieval process (Kopelman, 1992), but the detailed neural mechanisms of this process are not well understood.

Norepinephrine (NE)-containing neurons in the brain are divided into discrete cell groups in the pons and medulla, projecting to a diverse array of brain regions (Robertson et al., 2013; Chandler et al., 2014). NE plays a key role in the modulation of long-lasting synaptic potentiation and strengthening in the hippocampus (Huang and Kandel, 1996; Gelinas and Nguyen, 2005; O'Dell et al., 2010) and amygdala (Huang et al., 2000; Huang and Kandel, 2007; Johansen et al., 2014). Indeed, a number of behavioral studies have demonstrated that the central NE system contributes to associative aversive memory processes, including acquisition (Bahar et al., 2003; Bush et al., 2010; Ferry et al., 2015), consolidation (Guzmán-Ramos et al., 2012; LaLumiere et al., 2003), and reconsolidation (Kobayashi et al., 2000; Zhou et al., 2015; Villain et al., 2016).

By contrast, studies of the NE system in the retrieval process with different behavioral tasks have produced controversial results. Electrical stimulation of the locus coeruleus (LC), the major NE cell group in the brain (Robertson et al., 2013; Chandler et al., 2014), enhances performance in a complex maze task during a retention test, which is blocked by administration of a β-adrenergic receptor antagonist (Sara and Devauges, 1988; Devauges and Sara, 1991). A genetic study using dopamine β-hydroxylase knock-out mice showed that NE is involved in the retrieval of a particular type of contextual and spatial memory dependent on the hippocampus (Murchison et al., 2004). However, application of a β-adrenergic receptor antagonist into the amygdala does not influence the retrieval of conditioned flavor aversion requiring amygdalar function (Miranda et al., 2007). Therefore, the exact role of the central NE system in memory retrieval remains unclear.

In this study, we address the role of NE neurons, focusing on the LC in the retrieval process of conditioned taste aversion. To activate specific neuronal types, we developed a novel chemogenetic approach that uses olfactory ionotropic receptors (IRs) from *Drosophila melanogaster* (Benton et al., 2009; Rytz et al., 2013; van Giesen and Garrity, 2017). IRs typically comprise heteromeric complexes of a "tuning" receptor, which defines ligand specificity, and an obligate coreceptor. In this work, we exploited the well characterized complex of the tuning receptor IR84a and the coreceptor IR8a, which confers excitatory responsiveness to the aromatic ligands phenylacetaldehyde (PhAl) and phenylacetic acid (PhAc) when expressed in heterologous cell types (Benton et al., 2009; Abuin et al., 2011; Grosjean et al., 2011). This approach, which we have named "IR-mediated neuronal activation" (IRNA), enables efficient and sustained stimulation of the target neurons (Fig. 1*A*). The IRNA technology enabled the activation of LC NE neurons expressing the IR84/IR8a complex in response to exogenous ligands, and the resultant stimulation of NE release enhanced the retrieval of conditioned memory for taste. This role of the LC NE neurons in memory retrieval was mediated, in part, through α_1- and β-adrenergic receptors in the basolateral nucleus of the amygdala (BLA). Pharmacological inhibition of LC NE neurons confirmed the facilitative role of these neurons in memory retrieval through the LC–BLA pathway via adrenergic receptor subtypes.

Materials and Methods

Animals

A gene cassette was constructed, in which IR84a fused to enhanced green fluorescent protein (GFP) with a human calreticulin signal peptide was connected to IR8a via a 2A peptide (GFP-IR84a-2A-IR8a). The GFP-IR84a-2A-IR8a cassette was exchanged by the GFP cDNA part of the plasmid pTH-GFP that contained a 9 kb rat tyrosine hydroxylase (TH) gene promoter, rabbit β-globin second intron, GFP cDNA, and rabbit β-globin and SV40 early gene polyadenylation signals (Sawamoto et al., 2001; Matsushita et al., 2002), resulting in the plasmid pTH-GFP-IR84a/IR8a (Fig. 1*B*). The transgene construct was linearized by SalI digestion, purified by gel electrophoresis, and microinjected into fertilized C57BL/6J mouse eggs, which were then implanted into pseudopregnant females. Transgenic (Tg) mice were identified by Southern blot hybridization or PCR with genomic DNA prepared from tail clips.

We generated 25 independent Tg founders carrying the TH-GFP-IR84a/IR8a transgene. The Tg offspring derived from each founder were subjected to GFP immunostaining with sections prepared from the transgenic brain. Expression levels and distribution of the transgene in the brain regions, including the olfactory bulb, ventral midbrain, and hindbrain, showed variations among the strains. Based on the specificity and level of transgene expression, we selected one Tg strain, termed the TH-GFP-IR84a/IR8a-2–1. This strain was used for the following experiments in the present study.

Animal care and handling procedures were conducted in accordance with the guidelines established by the Laboratory Animal Research Center of Fukushima Medical University. All procedures were approved

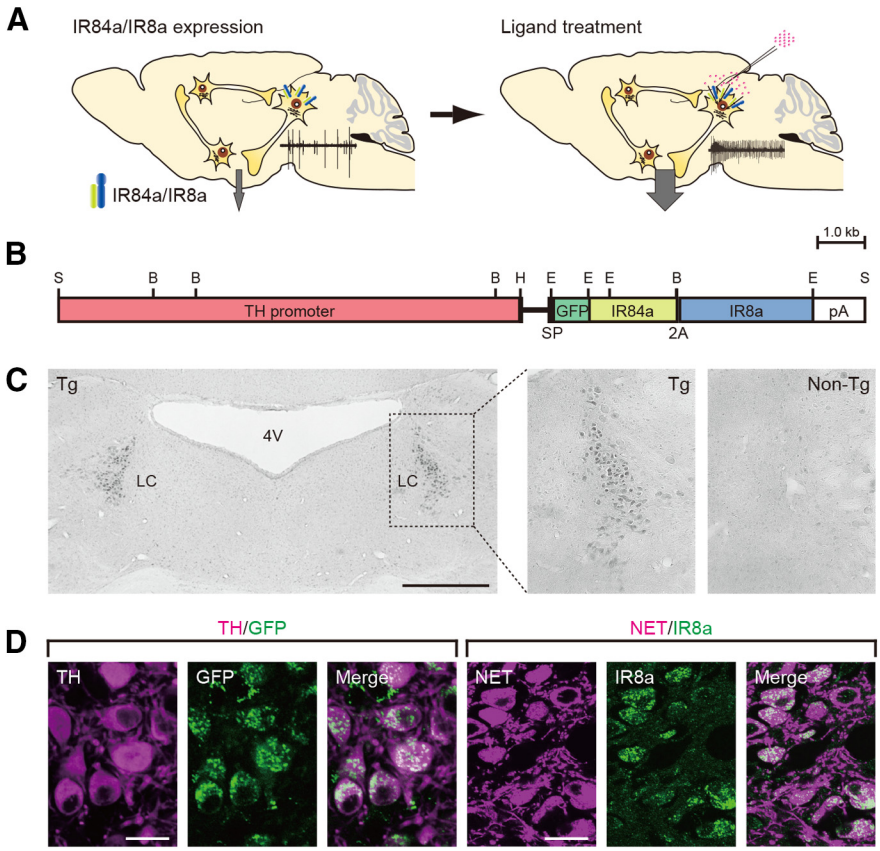

Figure 1. Experimental strategy and transgene expression. ***A***, Strategy for IRNA. The Tg mice expressing IR84a/IR8a genes in specific cell types are treated with exogenous ligands in the brain regions, resulting in the activation of target neurons. ***B***, Structure of the gene cassette encoding GFP-IR84a-2A-IR8a with a signal peptide (SP) downstream of the TH gene promoter. B, *Bam*HI, E, *Eco*RI, H, *Hind*III, S, *Sal*I; pA, polyadenylation signal. ***C***, Transgene expression in the LC revealed by GFP immunohistochemistry. 4V, Fourth ventricle. ***D***, Confocal microscopic images of LC sections obtained from double immunohistochemistry for TH/GFP and NET/IR8a. Scale bars: ***C***, 500 μm; ***D***, 20 μm.

by the Fukushima Medical University Institutional Animal Care and Use Committee. Mice were maintained on a 12 h light/dark cycle (lights on at 7:00 A.M.) at an ambient temperature of 22°C. All experimental procedures were conducted during the light period. Mice aged 12–14 weeks old were used for the following experiments except for *in vitro* electrophysiology, in which mice 17–20 postnatal days of age were used. Male mice were used in all behavioral experiments. In *in vitro* electrophysiology experiments, mice were subjected to experiments without sex determination. In all other experiments, both males and females were used. Mice were housed in groups of three to five, and they were single housed after the stereotaxic surgeries for the microdialysis and behavioral experiments. The assignment of mice to the experimental conditions was random.

Vector transduction

Lentiviral vector pseudotyped with vesicular stomatitis virus glycoprotein (VSV-G) was prepared as described previously (Kato et al., 2007) with slight modifications. A part of the IR8a gene in the gene cassette GFP-IR84a-2A-IR8a was exchanged by gene encoding IR8a tagged by hemagglutinin (HA) peptide (termed GFP-IR84a-2A-HA-IR8a). The transfer plasmid contained the cDNA encoding GFP-IR84a-2A-HA-IR8a downstream of the murine stem cell virus promoter. The envelope plasmid contained VSV-G cDNA under the control of a cytomegalovirus enhancer/chicken β-actin promoter. HEK293 T cells were transfected with transfer, envelope, and packaging plasmids using the calcium phosphate precipitation method. Viral vector particles were pelleted by centrifugation at 6000 × *g* for 16–18 h and suspended in PBS. Different concentrations (55% and 20%) of sucrose in PBS and the particle solution were sequentially overlaid from the bottom of ultracentrifuge tubes. The tubes were centrifuged with a SW55Ti swinging-bucket rotor (Beckman Coulter) at 100,000 × *g* for 2 h. The viral vector layer was collected, dialyzed in PBS, and concentrated by centrifugation through a Vivaspin filter (Vivascience). Proper concentrations of viral vector were used for transduction of HEK293 T cells, and functional titer [transduction unit (TU)] was measured using flow cytometry (FACSCalibur, Becton Dickinson). HEK293 T cells (~5×10^5 cells in a 6 cm dish) were transduced with the lentiviral vector encoding GFP-IR84a-2A-HA-IR8a with a functional titer of ~2×10^8 TU/ml (4 μl), and were used for histologic and electrophysiological experiments.

Histology

Mice were anesthetized with sodium pentobarbital (50 mg/kg, i.p.) and perfused transcardially with PBS, followed by fixation with 4% paraformaldehyde in 0.1 M phosphate buffer, pH 7.4. Sections (30 μm thick) were incubated with a primary antibody for GFP (1:2000; rabbit, Thermo Fisher Scientific; RRID:AB_221570) and then with a biotinylated secondary antibody (1:500; anti-rabbit IgG, Jackson ImmunoResearch; RRID:AB_2340593). The immunoreactive signals were visualized by use of a Vectastain Elite ABC Kit (Vector Laboratories; RRID:AB_2336827) with 3,3'-diaminobenzidine tetrahydrochloride/H_2O_2 as a chromogen. For double-fluorescence immunohistochemistry, sections were incubated with anti-TH antibody (1:400; mouse, Millipore; RRID:AB_2201528) and anti-GFP antibody (1:2000; rabbit, Thermo Fisher Scientific; RRID:AB_221570) or antibody for NE transporter (NET; mouse, 1:2000) and anti-IR8a antibody (rabbit; 1 μg/ml). Anti-IR8a antibody was prepared by immunization with purified protein of glutathione *S*-transferase fused to a 27 aa fragment of IR8a (DKYSPYSSRNNRQAYPVACREFTLRES). The specificity of anti-IR8a antibody was confirmed by double-fluorescence immunohistochemistry for NET/IR8a with LC sections prepared from the Tg and non-Tg mice. The sections were incubated with species-specific secondary antibodies conjugated to Alexa Fluor 488 (RRID:AB_2535792; Molecular Probes) or Cy3 (Jackson ImmunoResearch; RRID:AB_2340813). Fluorescent images were visualized under a confocal laser-scanning microscope (LSM510 or LSM800, Zeiss) equipped with proper filter cube specifications.

For cell counts of double-fluorescence immunohistochemistry for TH and GFP, four sections through the LC along with the anteroposterior (AP) coordinates between −5.43 and −5.68 mm from bregma were prepared from each mouse and used for double immunostaining. The number of immunopositive cells in the region of interest (200 × 200 μm) was counted by using a computer-assisted imaging program (ImageJ version 1.62, National Institutes of Health), and the number of TH^+/GFP^+ cells was divided by that of total TH^+ cells in each section. The average of the percentage obtained from the sections was calculated. Four mice were used for cell counts of the immunostaining.

For double-fluorescence immunohistochemistry with cultured cells, HEK293 T cells were cultured overnight in a 6 cm dish with a cover glass. The cells on the glass were fixed with 4% paraformaldehyde in PBS and followed by incubation with anti-GFP antibody (1:2000; goat, Frontier Institute; RRID:AB_2571574) and anti-HA-tag antibody (1:1000; rabbit, Cell Signaling Technology; RRID:AB_1549585). The cells were then incubated with species-specific secondary antibodies conjugated to Alexa Fluor 488 (Thermo Fisher Scientific; RRID:AB_2534102) or Cy3 (Jackson ImmunoResearch; RRID:AB_2307443). Fluorescent images were taken as described above.

To validate the cytotoxicity of ligand treatment, sections through the LC were prepared from the Tg mice 7 d after unilateral treatment with PBS or PhAc (0.4/0.6%; Wako Pure Chemical) for the microdialysis analysis, and stained for TH and NET immunohistochemistry. The sections were incubated with anti-TH antibody (mouse, 1:1000) or anti-NET antibody (mouse, 1:500) and then with a biotinylated secondary antibody (1:200; anti-mouse IgG, Jackson ImmunoResearch; RRID:AB_2340785). The immunoreactive signals were visualized by use of a Vectastain Elite ABC Kit. The ratio of the number of cells stained for TH or NET in the treated side relative to the intact side was calculated. In the experiment for the staining with cell death markers, ibotenic acid (IBO; Sigma-Aldrich) was used as a positive control to detect cell death signals. Mice were anesthetized with 1.5% isoflurane and IBO (1 mg/ml) or PhAc (0.6%), injected stereotaxically into the LC (0.2 μl/site) in either hemisphere of the Tg mice using a borosilicate glass capillary (Sutter Instrument) with tapered tip (60 μm in diameter) connected to a 10 μl Hamilton syringe filled with PBS or IBO through a Teflon tube (EICOM). The coordinates from λ or dura were AP −0.75 mm, mediolateral (ML) +0.65 mm, and dorsoventral (DV) −2.5 mm, according to the mouse stereotaxic atlas (Franklin and Paxinos, 2008). Mice were decapitated 24 h later, and their brains were removed, flash frozen with dry-ice powder, and stored at −80°C until used. Terminal deoxynucleotidyl transferase-mediated biotinylated UTP nick end labeling (TUNEL) was performed following the manufacturer protocol (Takara; RRID:AB_2800362). For immunostaining with an antibody for activated caspase-3 (1:1000; rabbit, BD Biosciences; RRID:AB_397274) with counterstaining with DAPI (4′,6′-diamidino-2-phenylindole dihydrochloride; Thermo Fisher Scientific; RRID:AB_2629482), the LC sections were prepared from mice 3 d after the PBS or IBO treatment.

Electrophysiology

For slice electrophysiology, mice were anesthetized with 1.5% isoflurane. Coronal brain slices containing the LC were cut (300 μm thick) using a microslicer (PRO7, Dosaka) in ice-cold oxygenated cutting Krebs' solution of the following composition (mM): choline chloride 120, KCl 2.5, $NaHCO_3$ 26, NaH_2PO_4 1.25, D-glucose 15, ascorbic acid 1.3, $CaCl_2$ 0.5, and $MgCl_2$ 7. The slices were then transferred to a holding chamber containing standard Krebs' solution of the following composition (mM): NaCl 124, KCl 3, $NaHCO_3$ 26, NaH_2PO_4 1, $CaCl_2$ 2.4, $MgCl_2$ 1.2, and D-glucose 10, pH 7.4 when bubbled with 95% O_2/5% CO_2. Slices were incubated in the holding chamber at room temperature (21–26°C) for at least 1 h before recording. Neurons in the LC were visualized with a 60-× water-immersion objective attached to an upright microscope (BX50WI, Olympus Optics). LC neurons with fluorescence were visualized using the appropriate fluorescence filter (U-MWIG3, Olympus Optics). Patch pipettes were made from standard-walled borosilicate glass capillaries (Harvard Apparatus). For the recording of membrane potentials, a K-gluconate-based internal solution was used of the following composition (mM): K-gluconate 120, NaCl 6, $CaCl_2$ 5, $MgCl_2$ 2, K-EGTA 0.2, K-HEPES 10, Mg-ATP 2, and Na-GTP 0.3, pH adjusted to 7.4 with 1 M KOH. Whole-cell recordings were made from LC neurons with fluorescence using a patch-clamp amplifier (Axopatch 200B, Molecular Devices). Data were stored on digital audiotapes using a DAT recorder (DC to 10 kHz; Sony), and were digitized offline at 10 kHz (low-pass filtered at 2 kHz with an 8-pole Bessel filter) using pCLAMP9 software (Molecular Devices). NE cells in the LC were identified by low-frequency (<7 Hz) action potentials with large afterhyperpolarization, as described in previous studies (van den Pol et al., 2002; Zhang et al., 2010). The effects of PhAc (0.1%) on the membrane potential were assessed after they had reached a steady state (starting point), and the mean firing frequency and membrane potential were calculated during a 30 s test period before the drug application (pre) and after the starting point (post). Although a few neurons had a firing frequency >7 Hz (9–10 Hz) before drug application, these neurons were also included in the analyses because of the characteristic shape of action potentials with large afterhyperpolarization.

For cultured cell electrophysiology, ligand-induced currents were measured at room temperature using the standard whole-cell voltage-clamp technique (Osanai et al., 2006; Tarradas et al., 2013). Borosilicate glass pipettes (4–6 MΩ) were filled with an intracellular solution containing (mM) K-methanesulfonate 135, KCl 5, EGTA 0.5, Mg-ATP 5, Na-GTP 0.4, and HEPES 10, pH 7.2, adjusted with KOH, and were used for voltage-clamp recordings. Cells were continuously perfused with a modified Hanks solution containing (mM) NaCl 137, KCl 3, $MgCl_2$ 1.2, $CaCl_2$ 1.8, glucose 20, and HEPES 10, pH 7.4, adjusted with NaOH after dissolving PhAc. Currents were recorded with an EPC-10 amplifier (HEKA), and the data were sampled at 2 kHz. Nontransduced GFP^- cells were used for the controls. To monitor ligand dose responses, the amplitudes of the ligand-induced currents were measured at different doses of PhAc and normalized in each cell to the amplitude at the average of 0.01% PhAc treatment.

An extracellular single-unit recording was conducted *in vivo* (Takahashi et al., 2010). Mice were anesthetized with 1.5% isoflurane, and anesthesia was maintained with 0.5–1.0% isoflurane based on the monitoring of an electroencephalogram. Mice were placed in the stereotaxic frame (catalog #SR-5 M, Narishige) with ear bars and a mouth-and-nose clamp. Body temperature was maintained at 37–38°C with a heating pad. The scalp was opened, and a hole was drilled in the skull above the LC with the coordinates AP −1.2 mm and ML +0.9 mm from λ, according to the mouse stereotaxic atlas (Franklin and Paxinos, 2008). Two skull screws were placed over the occipital bone, and another skull screw was placed on the frontal bone. One of the two screws over the occipital bone was used as a reference for the recording. For pneumatic injection, the firing activity was recorded by a double-barrel glass pipette, in which the tip of the injection capillary (tip diameter, 50 μm; A-M Systems) was glued ~100 μm above the tip of the recording electrode (tip diameter, 2–3 μm; impedance, 15–20 MΩ; Harvard Apparatus). The pipette was lowered into the LC at DV −2.2 to −3.5 mm from dura, and recording was performed using Spike2 (Cambridge Electronic Design) at a sampling rate of 20 kHz. NE neurons were identified based on a slow tonic firing (<7 Hz) with long spike duration (>0.8 ms) as described previously (Takahashi et al., 2010). A solution of 1% PhAc was delivered into the LC through a pneumatic pump (model PV-820, World Precision Instruments). In this technique, a small amount of ligand solution (estimated at 4–10 nl) was infused through the pump (20–40 psi, for 10–100 ms). The mean firing rate was calculated for each neuron during a 30 s test period immediately before injection (pre) and after injection (post) and was used for comparisons. After the electrophysiological experiments, the recording sites were marked by iontophoretic injection of 2% Pontamine Sky Blue. Mice were deeply anesthetized with sodium pentobarbital and perfused transcardially with PBS, followed by 10% formalin. Brain sections were stained with neutral red for the verification of recording sites. The postmortem histologic analysis verified deposits of recording sites in the LC.

Microdialysis

Mice were anesthetized with 1.5% isoflurane and underwent unilateral stereotaxic surgery with a 25 gauge guide cannula (EICOM) for a dialysis probe aimed at the anterior cingulate cortex (ACC) or the BLA, as well as a 30 gauge guide cannula (EICOM) for microinjection into the LC at the ipsilateral side. The coordinates (mm) were AP +0.7, ML +0.3, and DV −0.4 for the ACC dialysis probe; AP −1.2, ML +3.5, DV −3.5 for the BLA dialysis probe (from bregma or dura); and AP −0.75, ML +0.65, and DV −2.5 for the LC microinjection (from λ or dura), according to the mouse stereotaxic atlas (Franklin and Paxinos, 2008). Two or three days later, the stylet in the cannula was replaced with an active membrane dialysis probe (1.0 mm in length; 0.22 mm in outer diameter; EICOM) that was connected to a 2500 μl syringe filled with artificial CSF (aCSF) of the following composition (mM): NaCl 148, KCl 4.0, $MgCl_2$ 0.85, and $CaCl_2$ 1.2. For the intra-LC injection, the stylet in the LC cannula was replaced with a 35 gauge internal cannula (1 mm beyond the tip of the implanted guide cannula; EICOM) connected to a 10 μl Hamilton syringe, aCSF was pumped through the probe at a rate of 1.0 μl/min for 2 h, and dialysis samples were collected every 30 min using a refrigerated fraction collector (model EFC-82, EICOM). Each sample vial contained 10 μl of antioxidant, which consisted of 20 mM phosphate buffer, including 25 mM EDTA-2Na and 0.5 mM ascorbic acid, pH 3.5. Three baseline samples were collected to measure a tonic

level of NE. This was followed by PhAc (0.1/0.4/0.6%) or PBS injection into the LC for 5 min to a total volume of 0.2 μl. Four samples were collected thereafter to assess the time course for change in NE level after the injection. The amount of NE in each fraction was determined by a high-performance liquid chromatography system (2.1 × 150 mm; model CA-50DS, EICOM), with the mobile phase containing 5% methanol in 100 mM sodium phosphate buffer, pH 6.0) equipped with an electrochemical detector (model ECD-300, EICOM). Results are expressed as a percentage of baseline concentration (analyte concentration × 100/mean of the three baseline samples). After the microdialysis experiments, mice were deeply anesthetized with sodium pentobarbital and perfused transcardially with PBS, followed by 10% formalin. Brain sections were stained with neutral red for the verification of placement sites. The postmortem analysis confirmed the placement sites of the injection needle in the LC and dialysis probes in the ACC and the BLA.

Behavioral analysis

Taste reactivity tests were conducted as described previously (Inui et al., 2013; Yasoshima and Shimura, 2017) with some modifications. Mice were anesthetized with 1.5% isoflurane and bilaterally implanted with 26 gauge guide cannulae (Plastics One) into the LC using the following coordinates (mm): AP −0.9, ML +0.6, and DV −2.3 from λ or dura according to the brain atlas (Franklin and Paxinos, 2008). An intraoral catheter for infusion of the taste stimulus (0.5 M sucrose dissolved in tap water) was placed on the left side of the oral cavity, and the inlet of the catheter was fixed with acrylic cement on the guide cannula assembly. After a 1 week recovery period, mice were placed on a 20 h water deprivation schedule. Fluid intake training with tap water was conducted over 4 d. Consumption was measured by weighing bottles before and after the 20 min access. Mice were allowed to access water *ad libitum* for 3 h after the training. The taste aversion paradigm contained three different phases (see Fig. 5*A*). In the conditioning phase (days 1 and 2), mice were presented to 0.5 M sucrose with the spout as the conditioned stimulus (CS) for 20 min, and 10 min later, they received an intraperitoneal injection with 0.15 M lithium chloride (LiCl; 2% of body weight) as the unconditioned stimulus (US). In the habituation phase (days 3–5), mice were habituated to intraoral infusion with tap water in the test chamber. The chamber consisted of an acrylic cylinder (diameter, 140 mm; height, 250 mm) and an acrylic box (length and width, 325 mm; height, 310 mm) equipped with an inside mirror, which enabled monitoring of the behavior of mice from the bottom, and the infusion was conducted at the constant flow rate of 50 μl/min for 15 min by a syringe pump (EICOM). On the day of the test phase (day 6), a solution (0.2 μl/site) containing PhAc (0.4/0.6%) or PBS was injected into the bilateral LC 20 min before CS presentation. The solution was delivered through a 33 gauge internal cannula (1 mm beyond the tip of the implanted guide cannula; Plastics One) at a flow rate of 0.05 μl/min. Mice were placed in the test chamber and infused intraorally with 0.5 M sucrose. Behavior was recorded during a 10 min test period using a digital video camera, and the latency for the initiation of rejection responses (including gaping, chin rubbing, forelimb flailing, paw wiping, and CS dropping) was measured. Our taste reactivity tests with unconditioned mice that received the intraperitoneal injection of saline instead of LiCl ($n = 4$) indicated that they showed no rejection responses during a 10 min test period.

For the taste sensitivity test, mice received a bilateral implantation of guide cannulae into the LC. Mice were placed on a 20 h water deprivation schedule and conducted the intake training over 4 d. They received microinjection of PBS or 0.6% PhAc into the bilateral LC (0.2 μl/site) 20 min before the fluid presentation, and 0.5 M sucrose was presented to mice for 20 min and the sucrose consumption was measured.

To monitor hedonic responses, mice were bilaterally implanted with 26 gauge guide cannulae into the LC, and then with an intraoral catheter for infusion of the taste stimulus on the left oral cavity as described above. Mice were habituated to the intraoral infusion with tap water in the test chamber. A solution (0.2 μl/site) containing PBS or 0.6% PhAc was injected into the bilateral LC, and mice were placed in the test chamber and infused intraorally with 0.5 M sucrose 20 min later. Behavior was recorded using a digital video camera, and the latency for the initiation of hedonic responses (including tongue protruding and lateral tongue protruding) was measured.

To test aversive responses to quinine, mice received a bilateral implantation of guide cannulae into the LC and a unilateral placement of an intraoral catheter into the oral cavity. Mice were habituated to the intraoral infusion with tap water in the test chamber. A solution (0.2 μl/site) containing PBS or 0.6% PhAc was injected into the bilateral LC, and mice were placed in the test chamber and infused intraorally with 0.2 mM quinine 20 min later. Behavior was recorded, and the latency for the initiation of rejection responses was measured.

Before the pharmacological blocking experiment with adrenergic receptor antagonists, doses of adrenergic receptor antagonists infused into the BLA were checked that do not affect the taste reactivity in wild-type mice. Mice were implanted bilaterally with guide cannulae into the BLA using the coordinates (AP −1.2 mm, ML +3.5 mm, DV −2.5 mm from bregma or dura) according to the mouse brain atlas (Franklin and Paxinos, 2008) and one intraoral catheter on the oral cavity. A solution (0.2 μl/site) containing prazosin (0.1 or 0.5 μg/site; PRAZ, Sigma-Aldrich) or propranolol (0.4 or 2.0 μg/site; PROP, Sigma-Aldrich) was injected bilaterally through an internal cannula into the BLA, and then the taste reactivity test was performed as described above. For the blocking experiment, mice were further implanted with the bilateral LC guide cannulae using the same coordinates as above. A solution (0.2 μl/site) containing PRAZ (0.1 μg/site) or PROP (0.4 μg/site) was injected bilaterally through an internal cannula into the BLA 5 min before bilateral injection of 0.6% PhAc into the LC (0.2 μl/site) for the taste reactivity test.

For the pharmacological inhibition experiment of LC neuronal activity, mice were implanted bilaterally with guide cannulae into the LC and an intraoral catheter into the oral cavity as above. Solution (0.2 μl/site) containing clonidine (CLO; 10 and 25 ng/site; Sigma-Aldrich) was injected bilaterally through an internal cannula into the LC and tested for taste reactivity 20 min later. For the pharmacological recovery, mice were further implanted bilaterally with guide cannulae into the BLA using the same coordinates as above. A solution (0.2 μl/site) containing methoxamine (MET; 0.5 μg/site; Sigma-Aldrich) or isoproterenol (ISO; 1.25 μg/site; Sigma-Aldrich) was injected bilaterally through an internal cannula into the BLA 5 min after the bilateral intra-LC injection of CLO (10 ng/site) for the taste reactivity test.

Locomotor activity was measured with a movement analyzer equipped with photo-beam sensors (SV-10, Toyo Sangyou). The number of beam breaks was counted for every 10 min block. The total number of beam breaks during a 60 min test period was calculated to evaluate the spontaneous locomotor activity during the pretreatment (blocks −6 to −1) and the locomotor activity after PBS treatment (blocks 1–6) and 0.6% PhAc treatment (blocks 7–12).

Behaviors of mice were scored by the experimenters, who were blind to the treatment of mice. After all behavioral testing, mice were anesthetized with sodium pentobarbital and perfused transcardially with PBS, followed by 10% formalin. Brain sections were stained with cresyl violet for the verification of placement sites. Histologic examination confirmed the placement sites of internal cannulae within the target brain regions.

Experimental design

Slice electrophysiology. For frequency data, we performed a paired comparison between pre-ligand application versus post-ligand application (0.1% PhAc) in each genotype; for depolarization data, an unpaired comparison between the genotypes was performed (Fig. 2*E*). The mean firing frequency and membrane potential of the pre-ligand and post-ligand application periods (30 s each) were calculated for each cell from the Tg and non-Tg mice.

Cell culture electrophysiology. The maximum amplitude of the current during the ligand application was recorded at different doses of PhAc (0.01, 0.02, 0.05, and 0.1%) for each subjected cell. We performed an unpaired comparison between GFP^+ and GFP^- cells on the data obtained from 0.1% PhAc treatment, as well as a two-factorial experiment, GFP (positive or negative; between-subjects factor) × PhAc (concentration of applied PhAc; 0.01, 0.02, 0.05, and 0.1%; repeated

measures) on the normalized data to the amplitude at the average of 0.01% PhAc treatment in each cell (Fig. 2*G*,*H*).

In vivo electrophysiology. We performed a paired comparison between pre-ligand and post-ligand pneumatic infusion (1% PhAc) in each genotype (Fig. 3*C*). The mean firing rate was calculated for each neuron during a 30 s test period immediately before and after injection (pre-ligand and post-ligand application, respectively). In analyzing the firing rate of the cells outside the LC, similar pre–post paired comparisons were performed (Fig. 3*D*).

Microdialysis. We performed two-factorial experiments, Treatment (concentration of injected PhAc; between-subjects factor) × Time (repeated measure), for each genotype to examine the time course of the effects of LC treatment on NE release in the terminal regions, the ACC (Fig. 3*F*,*G*) and BLA (Fig. 3*I*). Each dialysis sample (fraction) was collected every 30 min, and three baseline fractions (before PBS or PhAc injection to the LC) and four test fractions following the LC treatment were analyzed.

Validation of the cytotoxicity of PhAc treatment. We performed a one-factorial experiment each, with the independent variable Treatment (PBS, 0.4% PhAc, and 0.6% PhAc; between-subjects factor), for TH and NET immunohistochemistry (Fig. 4*B*). Three sections through the LC were prepared from each Tg mouse that had been unilaterally treated with PBS, 0.4% PhAc, or 0.6% PhAc in the microdialysis experiment, and perfused 7 d later. The sections were stained for TH and NET immunohistochemistry. The number of immunopositive cells for TH or NET antibody in the treated LC was divided by the number of those cells in the intact LC in each section, and then the ratios were averaged in each mouse for analysis.

Ligand-induced LC activation and taste associative memory retrieval. We first performed one-factorial experiments, with the independent variable Treatment (PBS, 0.4% PhAc, or 0.6% PhAc; between-subjects factor), in each genotype to examine the dose-dependent effects of the LC treatment on the conditioned responses, latency of the aversive taste reactivity to the CS (Fig. 5*C*) or number of the aversive responses (Fig. 5*E*). Then, to exclude other possibilities against the effect of the LC activation on memory retrieval, we performed several subsequent experiments: an unpaired comparison of unconditioned sucrose intake between PBS-treated and 0.6% PhAc-treated mice in each genotype (Fig. 6*A*); an unpaired comparison of latency of the hedonic taste reactivity to the unconditioned sucrose between PBS-treated and 0.6% PhAc-treated Tg mice (Fig. 6*B*); an unpaired comparison of latency of the aversive taste reactivity to the unconditioned quinine between PBS-treated and 0.6% PhAc-treated Tg mice (Fig. 6*C*); and an unpaired comparison of locomotor activity (beam breaks) between the Tg and non-Tg mice in each 60 min test period with (PBS or 0.6% PhAc) and without the LC treatment (Pre; Fig. 6*D*).

Pharmacological blockade of enhanced memory retrieval by LC activation. We first performed a one-factorial experiment, with the independent variable Treatment (PBS, 0.1 and 0.5 μg/site PRAZ, as well as 0.4 and 2.0 μg/site PROP; between-subjects factor), using wild-type mice to determine the concentration of the adrenergic receptor blockers that did not affect the retrieval of conditioned taste aversion (latency of the conditioned taste reactivity) when the drugs were injected into the BLA (Fig. 7*A*). Based on these results, we performed one-factorial experiments with the independent variable Treatment (PBS, 0.1 μg/site PRAZ, or 0.4 μg/site PROP; between-subjects factor) in each genotype to examine the effects of adrenergic receptor blockade in the BLA followed by the PhAc injection into the LC on latency of the aversive taste reactivity to the CS (Fig. 7*B*). Furthermore, we performed, with another cohort of

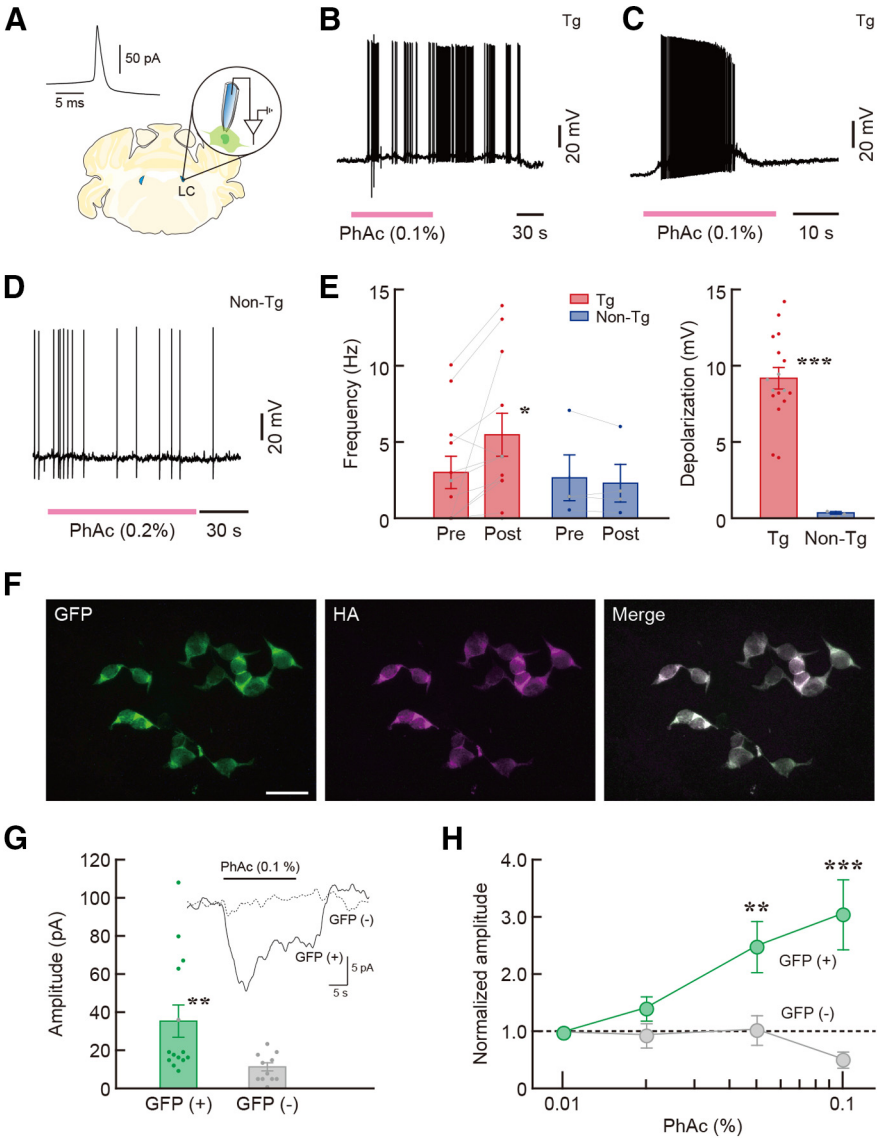

Figure 2. Ligand-induced LC activation in the Tg mice. ***A***, Schematic illustration of strategy for a whole-cell current-clamp recording of a brain slice preparation. Inset shows a typical waveform of NE neurons showing a wide action potential with large afterhyperpolarization. ***B***, Excitatory effect of 0.1% (7.3 mM) PhAc on the membrane potential of a NE neuron obtained from a Tg mouse. ***C***, Depolarization block after excitatory response to PhAc in another neuron in a Tg mouse. ***D***, Lack of effect of PhAc (0.2%) on the membrane potential of a neuron from a non-Tg mouse. ***E***, Bar graphs showing the firing frequency before (pre) and after (post) PhAc application and amplitude of PhAc-induced depolarization of NE neurons in the Tg ($n = 12$ for firing frequency and $n = 17$ for depolarization amplitude) and the non-Tg ($n = 4$) mice. $^{*}p < 0.05$ vs pretreatment in the Tg mice (paired two-tailed *t* test), $^{***}p < 0.001$ vs the non-Tg mice (unpaired two-tailed *t* test). ***F***, Expression of IR84a/IR8a complex in HEK293 T cells transduced by a lentiviral vector. Immunohistochemistry for GFP and HA tag detected expression of the two receptor subunits. Scale bar, 50 μm. ***G***, Bar graph showing the current amplitude in GFP^{+} ($n = 14$) and GFP^{-} ($n = 11$) cells. Inset shows mean current traces of the PhAc-induced inward current waveform. Solid and dotted lines indicate the waveform of GFP^{+} and GFP^{-} cells, respectively. $^{**}p < 0.01$ versus GFP^{-} cells. ***H***, Ligand dose responses of the GFP^{+} ($n = 12$) and GFP^{-} ($n = 8$) cells. The amplitudes of the ligand-induced currents were normalized in each cell to the amplitude at 0.01% PhAc. $^{**}p < 0.01$, $^{***}p < 0.001$ versus GFP^{-} cells at the corresponding ligand concentrations. Data are presented as the mean ± SEM. Individual data points are overlaid.

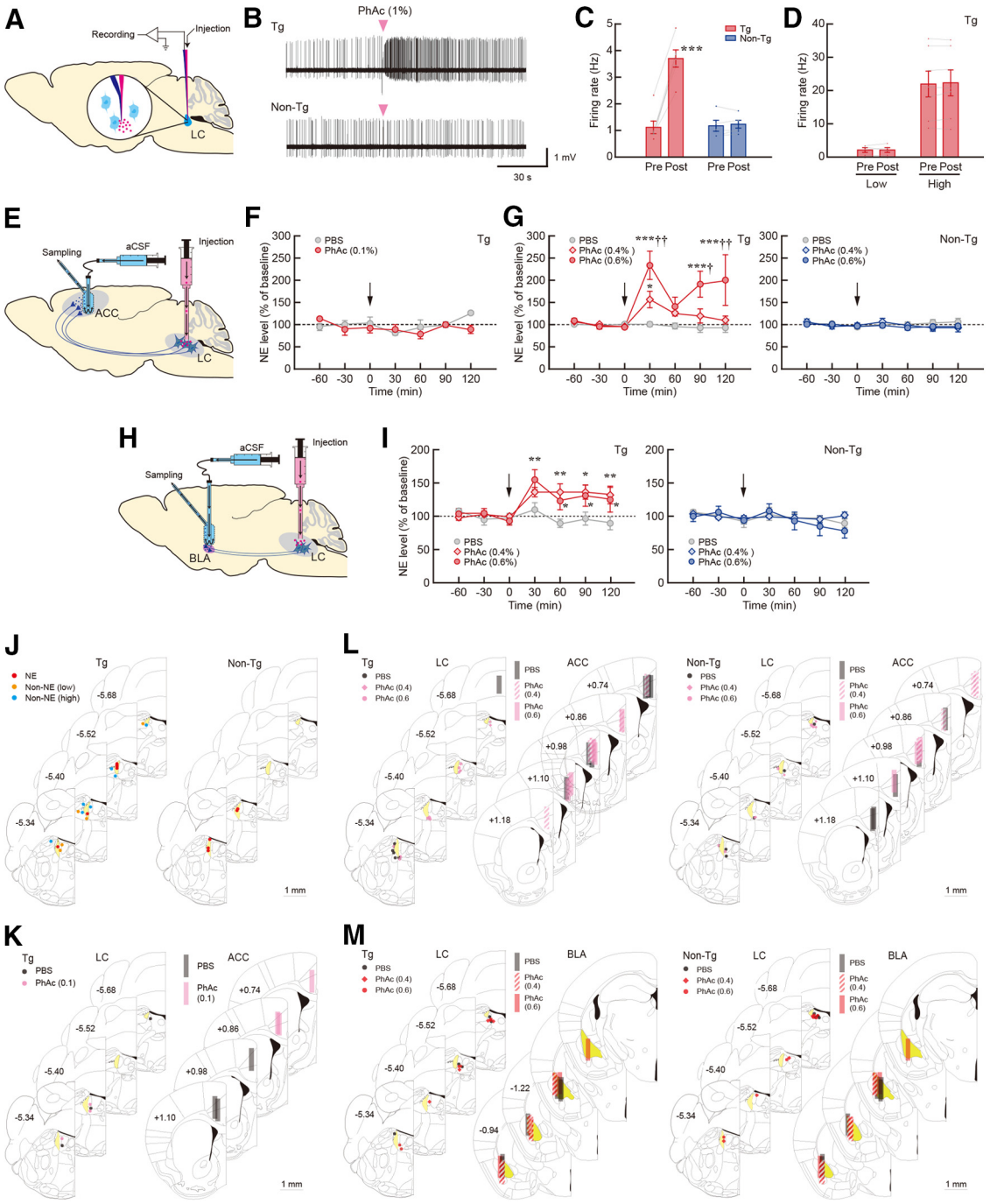

Figure 3. *In vivo* LC activation and increased NE release in the Tg mice. ***A***, Schematic diagram for the strategy of single-unit recording for *in vivo* electrophysiology. PhAc solution (1%) was pneumatically injected through a glass capillary attached to the recording electrode. ***B***, Firing pattern of an identified NE neuron in the Tg (top) and non-Tg (bottom) mice. The timing of the PhAc injection is indicated. ***C***, Firing rate in the pre- and post-PhAc injection period for the Tg ($n = 6$) and non-Tg ($n = 5$) mice. $^{***}p < 0.001$ (paired two-tailed t test). ***D***, Firing rate of non-NE neurons in the Tg mice with low and high frequency of the activity in the pre- and post-PhAc injection period ($n = 5$ or 7 for each type). ***E***, Diagram for the microdialysis for measuring NE release in the ACC in response to LC activation. PhAc solution or PBS was injected into the LC, and dialysis samples were collected from the ACC. ***F***, ***G***, Changes in the extracellular NE level after injection for PhAc (0.2 μl/site) of 0.1% in the Tg mice (***F***) and 0.4%/0.6% in the Tg and non-Tg mice (***G***). NE levels are expressed as a percentage of the average baseline levels of each mouse. $n = 3$ for the 0.1% PhAc experiment, and $n = 5$ or 6 for each group of the 0.4% and 0.6% PhAc experiments. $^{*}p < 0.05$, $^{***}p < 0.001$ versus PBS; $^{\dagger}p < 0.05$, $^{\dagger\dagger}p < 0.01$ versus 0.4% PhAc (Holm–Bonferroni test). ***H***, Diagram for the microdialysis for monitoring NE release in the BLA in response to LC stimulation. PhAc solution or PBS was injected into the LC, and dialysis samples were collected from the BLA. ***I***, Changes in the extracellular NE level after 0.4%/0.6% PhAc injection (0.2 μl/site) in the two kinds of mice. NE levels are expressed as a percentage of the average baseline levels of each mouse. $n = 5$ or 6 for each group. $^{*}p < 0.05$, $^{**}p < 0.01$ versus PBS (Holm–Bonferroni test). Data are presented as the mean ± SEM. ***J***, Placement sites of the recording electrodes (NE and non-NE neurons with low and high frequency) for *in vivo* electrophysiology. ***K***, ***L***, Placement sites of the injection needles into the LC and dialysis probes into the ACC after treatment with PBS and PhAc of 0.1% (***K***) or 0.4%/0.6% (***L***). ***M***, Placement sites of the injection needles into the LC and dialysis probes into the BLA after treatment with PBS and PhAc (0.4%/0.6%). The AP coordinates (in mm) are shown. Scale bar, 1 mm.

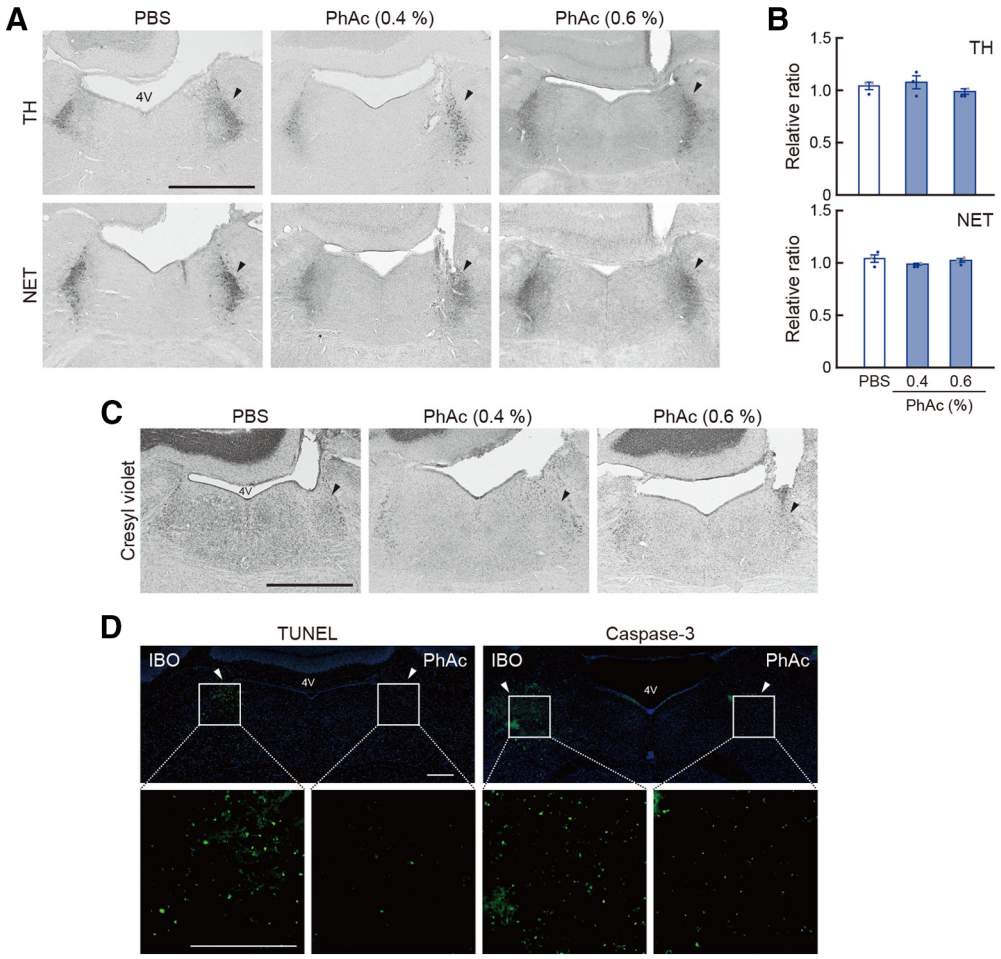

Figure 4. Morphologic analysis of LC neurons after PhAc stimulation. ***A***, Histology of LC NE neurons in the Tg mice after PhAc treatment. Sections through the LC were prepared from the Tg mice used for microdialysis analysis 7 d after unilateral treatment with PBS or PhAc (0.4/0.6%) and stained for TH and NET immunohistochemistry. ***B***, Cell counts for TH- and NET-immunopositive cells. The ratio of the number of cells stained for TH or NET in the treated side relative to the intact side was calculated. Data are presented as the mean ± SEM. Individual data points are overlaid. ***C***, Staining of LC sections with cresyl violet, showing no cell damage against LC neurons in the PhAc-treated side. ***D***, Staining for cell death markers. IBO (1 mg/ml) or PhAc (0.6%) was unilaterally injected into the LC (0.2 μl/site) of the Tg mice. LC sections were stained with TUNEL or immunohistochemistry for activated caspase-3. The LC areas in the top images were fourfold magnified in the lower images. Arrowheads indicate the injection sites into the LC. 4V, Fourth ventricle. Scale bars: ***A***, ***C***, ***D***, 1 mm.

the Tg mice, a one-factorial experiment with the independent variable Treatment (PBS, 0.1 μg/site PRAZ, or 0.4 μg/site PROP; between-subjects factor) on locomotor activity to determine whether the BLA treatments followed by LC PhAc injection affected the general activity of the Tg mice (Fig. 7*C*).

Pharmacological LC inhibition and taste associative memory retrieval. We first performed a one-factorial experiment, with the independent variable Treatment (PBS, 10 and 25 ng/site CLO; between-subjects factor), using wild-type mice to determine the concentration of the α_2-adrenergic receptor agonist that increased latency of the conditioned taste reactivity when the drug was injected into the LC (Fig. 8*A*). We also performed a one-factorial experiment with the independent variable Treatment (PBS, 10 and 25 ng/site CLO: between-subjects factor) on locomotor activity to determine whether the LC treatments affected the general activity of mice (Fig. 8*B*). Based on the results, we performed one-factorial experiments, with the independent variable Treatment (PBS, 0.5 μg/site MET, or 1.25 μg/site ISO; between-subjects factor), using wild-type mice to examine the effects of the adrenergic receptor agonists injected into the BLA following LC CLO treatment on latency of the aversive taste reactivity to the CS (Fig. 8*C*).

Statistical analysis

Although no statistical methods were used to predetermine the sample size for each measure, we used similar sample sizes to those that were reported in previous publications from our laboratories, which are generally accepted in the field. In each testing session, we conducted an experiment in two to five separate cohorts, each of which was designed to include all experimental groups. Data obtained across cohorts were pooled, and outliers were defined as data points located outside the range of mean ± 2 SDs. All parametric tests, paired *t* test, unpaired *t* test, one-way ANOVA, and two-way ANOVA were performed in a two-tailed manner using SPSS version 25 (IBM; RRID:SCR_002865). The reliably of the results was assessed against a type I error (α) of 0.05. Before the unpaired *t* test, we assessed equality of variances for two groups with a Levene's test, and if this was not the case, we reported the statistics (*F* and *p*) and then corrected the degree of freedom according to Welch's method. For significant effects identified in one-way ANOVAs, *post hoc* comparisons were performed with the Tukey HSD test to retain the prescribed familywise error rate α. For significant interactions revealed in two-way ANOVAs, *t* tests with Holm–Bonferroni sequential correction were used as *post hoc* analyses. When nonparametric tests were required, we performed the Mann–Whitney test using SPSS version 25. One (*), two (**), and three (***) asterisks in figures represent *p* values <0.05, 0.01, and 0.001, respectively.

Results

Insect IR-mediated stimulation of LC NE neurons

IRs constitute a family of sensory ligand-gated ion channels distantly related to ionotropic glutamate receptors that mediate

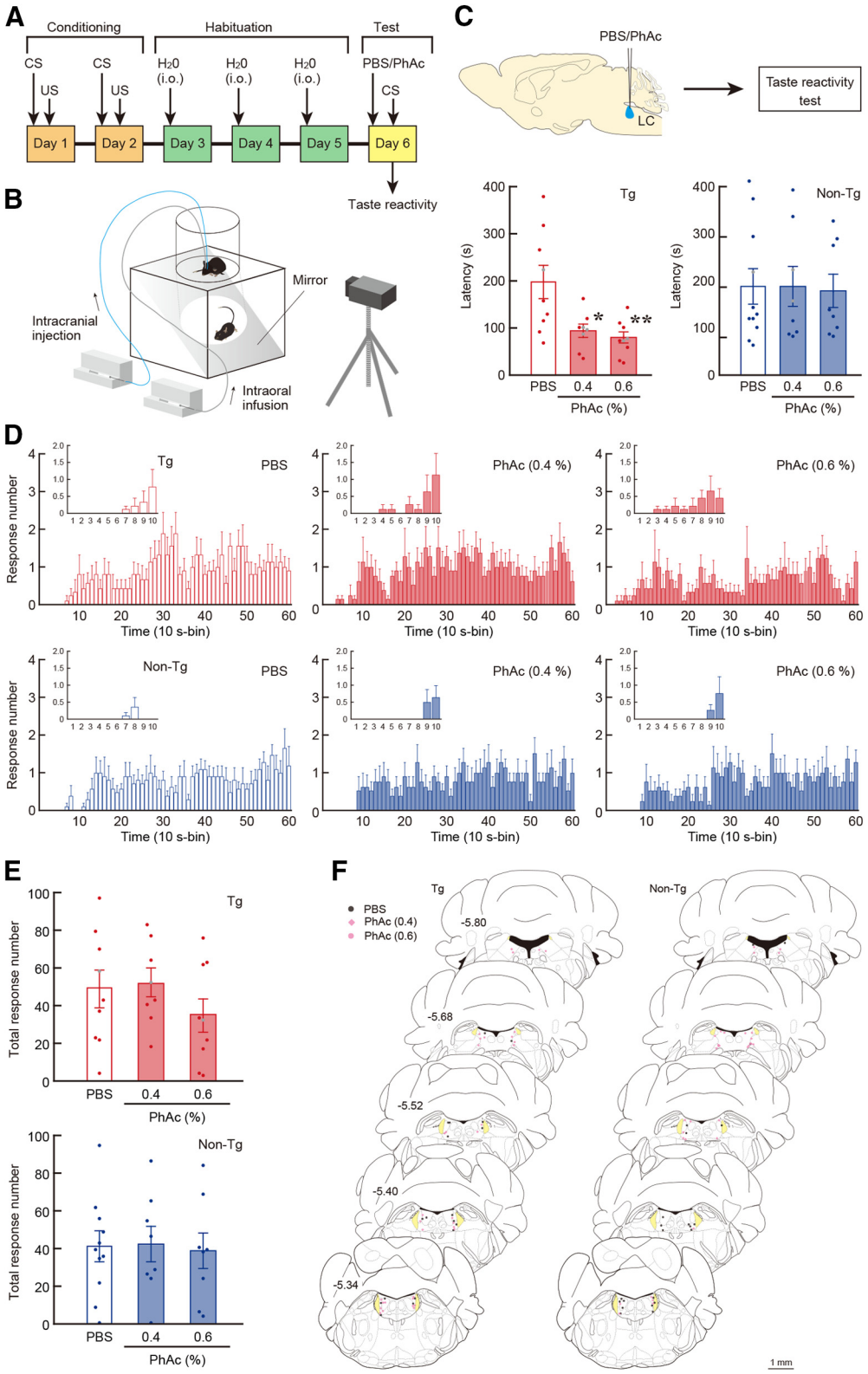

Figure 5. Ligand-induced LC activation enhances memory retrieval of conditioned taste aversion. ***A***, Schedule of the taste reactivity test. In the conditioning phase, mice were presented 0.5 M sucrose as the CS, followed by an intraperitoneal injection with 0.15 M LiCl as the US (days 1 and 2). Then, the mice were habituated to intraoral (i.o.) infusion with tap water in the test chamber (days 3–5). During the test phase, mice received a bilateral LC injection (0.2 μl/site) of PBS or solution containing PhAc (0.4/0.6%) followed by CS presentation to evaluate the rejection response (day 6). ***B***, Experimental apparatus used for the taste reactivity test. A mouse was placed in the test chamber and infused intraorally through a syringe pump, and the behavior of the animal was monitored from the bottom through an inside mirror using a digital video camera. ***C***, Taste reactivity test showing shorter latency of rejection response by ligand-induced LC activation in the Tg mice. $n = 8$ or 9 for each group in the Tg mice. $n = 8$–11 for each group in the non-Tg mice. *$p < 0.05$, **$p < 0.01$ versus PBS in the Tg mice (Tukey's HSD test). ***D***, Time course of aversive response number. Rejection responses during the 10 min test period were counted, and the number of responses at a 10 s bin was divided by the number of mice used in each group. Insets show the response number during the early phase (<100 s). ***E***, Total number of aversive responses during the 10 min test. Data are presented as the mean ± SEM. Individual data points are overlaid. ***F***, Placement sites of the injection needles into the LC (PBS and 0.4%/0.6% PhAc) for the taste reactivity test. The AP coordinates (in mm) are shown. Scale bar, 1 mm.

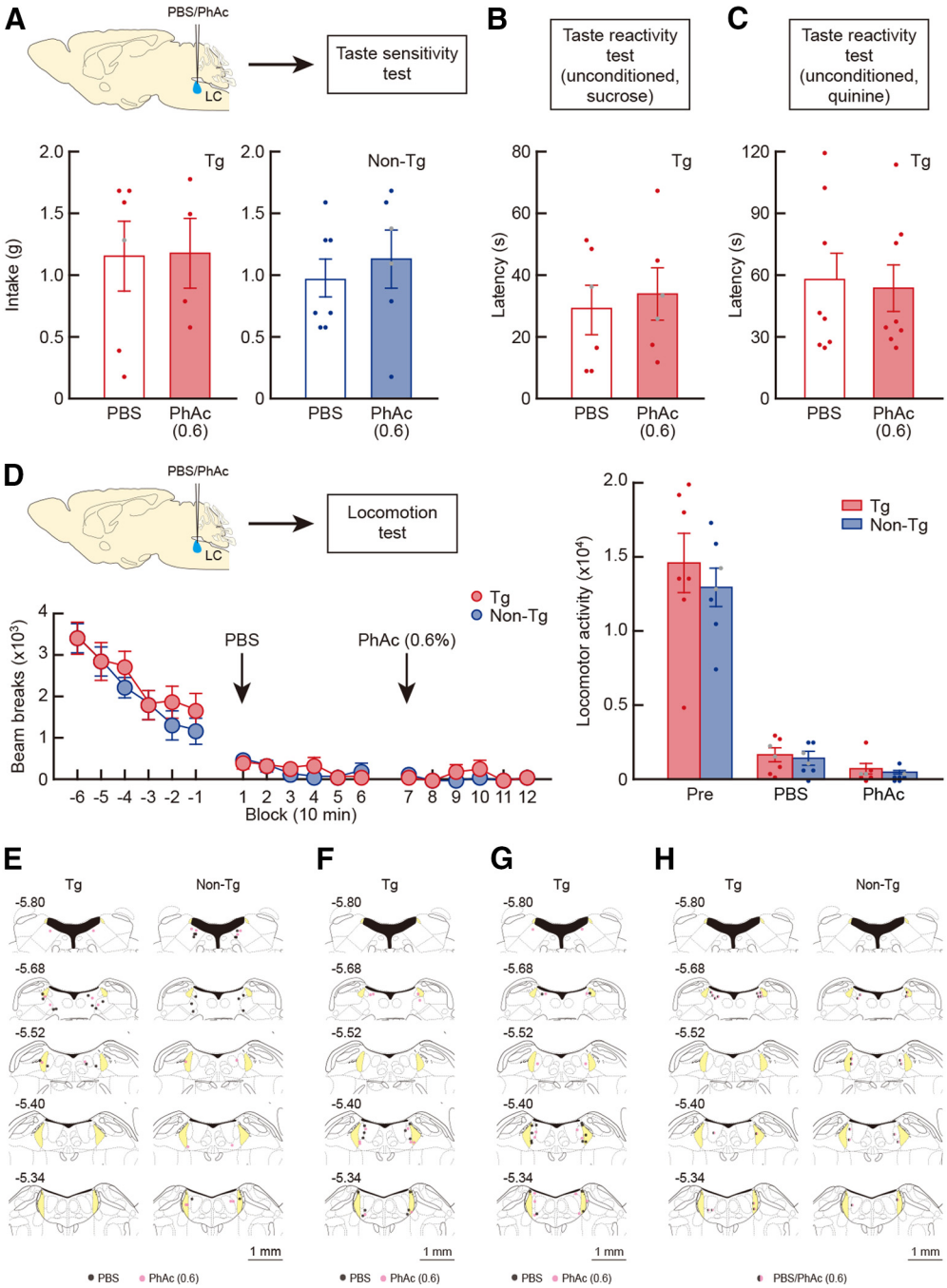

Figure 6. LC activation does not influence taste sensitivity, general arousal state, and locomotion. ***A***, Taste sensitivity test presenting normal intake of 0.5 M sucrose in unconditioned mice. PBS or PhAc solution (0.6%) was bilaterally injected into the LC (0.2 µl/site), and the fluid intake of 0.5 M sucrose was measured. $n = 4–7$ for each group. ***B***, Taste reactivity test showing normal hedonic responses to 0.5 M sucrose in unconditioned Tg mice. PBS or PhAc solution (0.6%) was bilaterally injected into the LC, and the latency for hedonic responses was measured. $n = 6$ for each group. ***C***, Taste reactivity test displaying unaltered aversive responses to 0.2 mM quinine in unconditioned Tg mice. After intra-LC injection of PBS or PhAc solution (0.6%), the latency for rejection responses was measured. $n = 8$ for each group. ***D***, Locomotor activity. The number of beam breaks was counted for every 10 min block. The total number of beam breaks during a 60 min test period was calculated as locomotor activity during the pretreatment (Pre; blocks −6 to −1) and after PBS treatment (blocks 1–6) and the following 0.6% PhAc treatment (blocks 7–12). $n = 7$ for each group. Data are presented as the mean ± SEM. Individual data points are overlaid. ***E–H***, Placement sites of the injection needles into the LC (PBS and 0.6% PhAc) for the taste sensitivity test (***E***), taste reactivity test for hedonic responses (***F***), taste reactivity test for aversive responses (***G***), and locomotion test (***H***). The AP coordinates (in mm) are shown. Scale bar, 1 mm.

environmental chemical detection in *Drosophila melanogaster* and other insects (Benton et al., 2009; Rytz et al., 2013; van Giesen and Garrity, 2017). The IR84a/IR8a heteromeric complex displays excitatory cellular responsiveness to the ligands PhAl and PhAc when expressed in heterologous neurons and *Xenopus* oocytes (Abuin et al., 2011; Grosjean et al., 2011). We took advantage of the known ligand specificity and functional autonomy of this complex to establish the IRNA method (Fig. 1*A*). Here, IR84a/IR8a genes are coexpressed under the control of a cell type-specific gene promoter, and the target neurons are stimulated with exogenous ligands. To express the receptors in NE neurons, we generated Tg mice carrying a GFP-IR84a-2A-IR8a gene construct downstream of the TH gene promoter (Sawamoto et al., 2001; Matsushita et al., 2002; Fig. 1*B*).

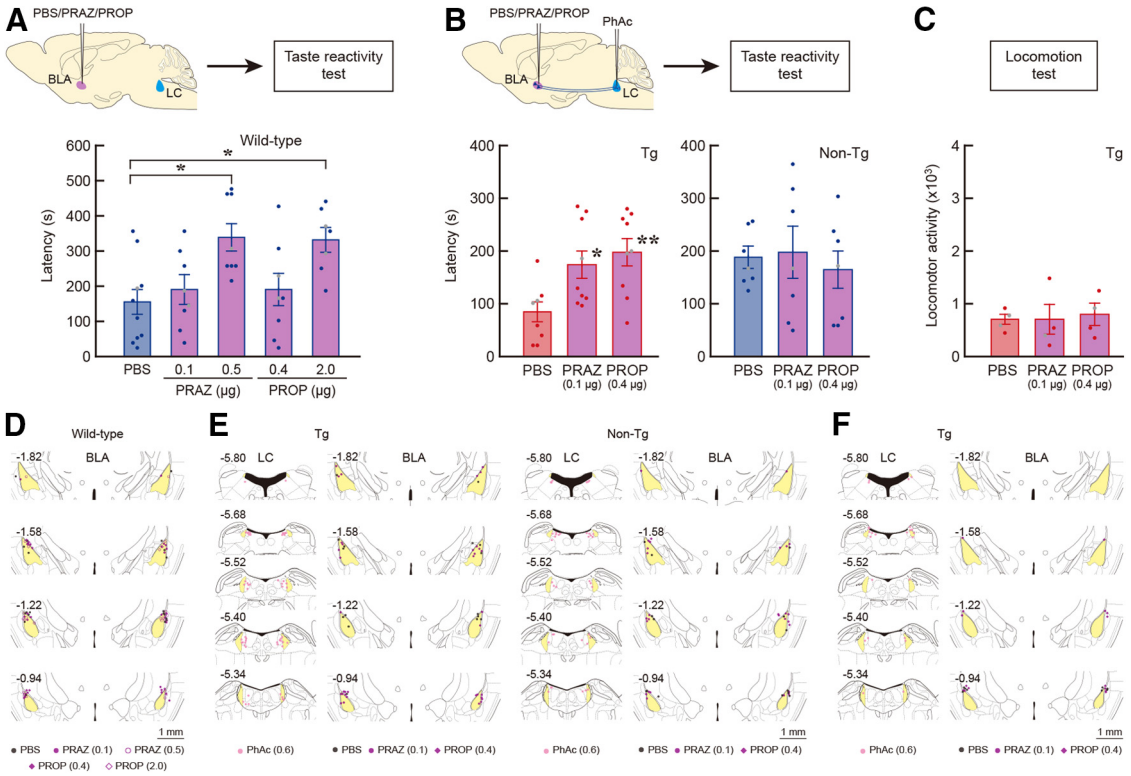

Figure 7. Pharmacological blockade of enhanced memory retrieval by LC activation. ***A***, Taste reactivity test in wild-type mice that received an intra-BLA infusion of PRAZ (0.1 or 0.5 μg/site) and PROP (0.4 or 2.0 μg/site). $n = 7$–10 for each mouse group. *$p < 0.05$ versus PBS infusion (Tukey's HSD test). ***B***, Taste reactivity test showing the blockade of shortened response latency in the LC-activated Tg mice by the intra-BLA infusion of PRAZ and PROP at the lower doses (0.1 and 0.4 μg/site, respectively). $n = 8$ or 9 for each group in the Tg mice. $n = 7$ for each non-Tg group. *$p < 0.05$, **$p < 0.01$ versus PBS in the Tg mice (Tukey's HSD test). ***C***, Locomotion test of the Tg mice that received the microinjection of PhAc (0.6%) into the LC and infusion of PRAZ and PROP (0.1 and 0.4 μg/site, respectively) into the BLA. After the habituation to the open field, the mice received the drug treatments, and then the total number of beam breaks (locomotor activity) during a 60 min period was monitored. $n = 4$ for each group in the Tg mice. Data are presented as the mean ± SEM. Individual data points are overlaid. ***D***, Placement sites of the injection needles into the BLA (PBS, PRAZ of 0.1 and 0.5 μg/site, and PROP of 0.4 and 2.0 μg/site) for the taste reactivity test. ***E***, ***F***, Placement sites of the injection needles into the LC (0.6% PhAc) and BLA (PBS, 0.1 μg/site PRAZ, and 0.4 μg/site PROP) for the taste reactivity test (***E***) and locomotion test (***F***). The AP coordinates (in mm) are indicated. Scale bar, 1 mm.

Immunostaining for GFP revealed transgene expression in LC neurons in the TH-GFP-IR84a/IR8a mouse line, whereas there was no expression in non-Tg littermates (Fig. 1*C*). Transgene expression was also observed in other catecholamine-containing cell groups (data not shown). In the Tg mice, GFP-IR84a expression was colocalized with TH immunoreactivity, and IR8a reactivity was colocalized with signals for NET (Fig. 1*D*). Double immunostaining for TH and GFP showed that almost all LC neurons express these receptors (93.6 ± 0.02% TH^+/GFP^+ cells/total TH^+ cells; $n = 4$).

To examine the cellular responsiveness of LC NE neurons expressing IR84a/IR8a, we performed a whole-cell current-clamp recording in slice preparations (Fig. 2*A*). NE cells in the LC were identified by a low firing frequency (<7 Hz) and wide action potentials with large afterhyperpolarization, as observed in previous studies (van den Pol et al., 2002; Zhang et al., 2010). In *Drosophila*, robust activation of IR84a/IR8a-expressing cells was induced by treatment with 0.1% (8.3 mM) PhAl (Abuin et al., 2011). For bath application in slices, we used a 0.1% (7.3 mM) solution of PhAc because of its higher water solubility compared with PhAl. The application of 0.1% PhAc depolarized the membrane of LC NE neurons in the Tg mice, increasing the firing frequency (Fig. 2*B*). In 5 of 17 neurons examined, the firing stopped after depolarization had reached its steady state even in the presence of PhAc (Fig. 2*C*), indicating the occurrence of depolarization block of these neurons. In the non-Tg mice, PhAc had little or no effect on the firing frequency or membrane potential of LC neurons (Fig. 2*D*). Excluding the neurons showing depolarization block, the firing frequency in the Tg mice was significantly elevated from 3.04 ± 1.04 Hz (pre) to 5.47 ± 1.38 Hz (post) by the PhAc application (Fig. 2*E*; $n = 12$; paired two-tailed t test, $t_{(11)} = 2.667$, $p = 0.0219$). This elevation persisted for 87.4 ± 21.7 s ($n = 12$). In the non-Tg mice, the frequency was similar between pre-PhAc and post-PhAc application (2.63 ± 1.48 and 2.35 ± 1.25 Hz, respectively; Fig. 2*E*; $n = 4$, paired two-tailed t test, $t_{(3)} = 1.011$, $p = 0.3864$). The amplitude of PhAc-induced depolarization in the Tg mice was 9.25 ± 0.69 mV and was significantly greater compared with the non-Tg value (0.34 ± 0.08 mV; Fig. 2*E*; Levene's test, $F_{(1,20)} = 5.060$, $p = 0.0365$; unpaired two-tailed t test with Welch's method, $t_{(16.42)} = 12.92$, $p < 0.0001$). These data indicated that application of the exogenous ligand in slices induced excitatory cellular responsiveness of LC NE neurons expressing IR84a/IR8a.

To confirm this ligand-specific reaction of the receptors in mammalian cultured cells, we generated a lentiviral vector encoding GFP-IR84a-2A-HA-IR8a to express the IR84a/IR8a complex. HEK293 T cells were transduced with the lentiviral vector, and the expression of the two receptors was detected by double immunostaining for GFP and HA tag (Fig. 2*F*). A whole-cell voltage-clamp experiment indicated that the application of 0.1% PhAc induced an inward current of GFP^+ cells expressing the receptor complex (Fig. 2*G*). The mean amplitudes in GFP^+ and GFP^- cells were 35.77 ± 7.91 pA ($n = 14$) and 11.14 ± 2.19 pA ($n = 11$), respectively, showing a significant increase of the

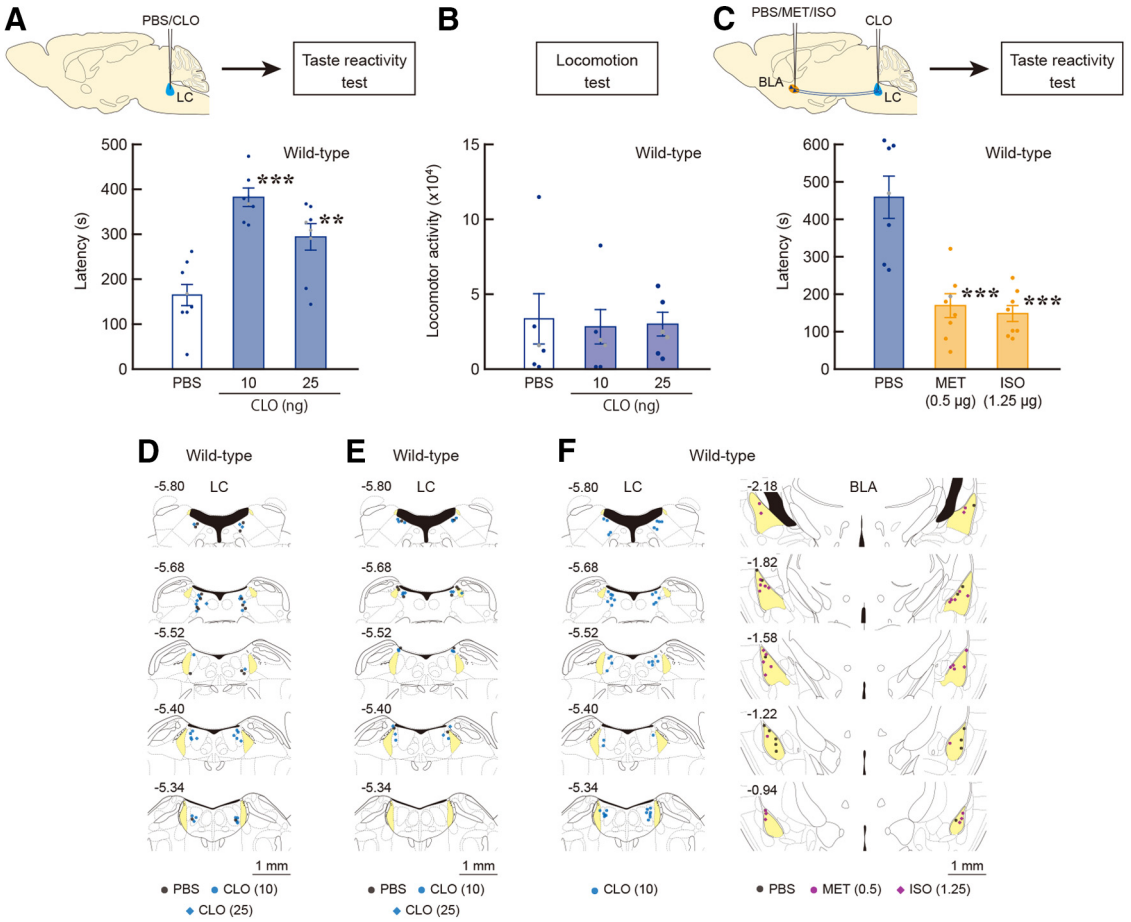

Figure 8. Pharmacological inhibition of LC neurons impairs memory retrieval. ***A***, Taste reactivity test showing the lengthened latency of rejection response in wild-type mice by injection of an α_2-adrenergic receptor agonist CLO (10 and 25 ng/site) into the LC. $n = 7$–8 for each mouse group. $^{**}p < 0.01$, $^{***}p < 0.001$ versus the PBS-treated mice (Tukey's HSD test). ***B***, Locomotion test of the wild-type mice injected with CLO (10 and 25 ng/site) in the LC. Total number of beam breaks (locomotor activity) during a 60 min period after the habituation was measured. $n = 6$ for each group. ***C***, Restoration of delayed rejection response in the CLO (10 ng/site)-injected mice by intra-BLA infusion of adrenergic receptor agonists MET (0.5 μg/site) and ISO (1.25 μg/site). $n = 8$ for the MET- and ISO-treated groups; $n = 7$ for the PBS-treated group. $^{***}p < 0.001$ versus the PBS-treated mice (Tukey's HSD test). Data are presented as the mean ± SEM. Individual data points are overlaid. ***D***, ***E***, Placement sites of the injection needles into the LC (PBS and CLO of 10 and 25 ng/site) for the taste reactivity test (***D***) and locomotion test (***E***). ***F***, Placement sites of the injection needles in the LC (10 ng/site CLO) and BLA (PBS, 0.5 μg/site MET, and 1.25 μg/site ISO) for the taste reactivity test. The AP coordinates (in mm) are presented. Scale bar, 1 mm.

amplitude in GFP^+ cells over GFP^- cells (Fig. 2*G*; Mann–Whitney U test = 28.00, $p = 0.0073$). To check ligand dose responses, different concentrations of PhAc were applied for the cultured cells. PhAc-induced current responses were specific to GFP^+ cells and displayed dose dependency (Fig. 2*H*; two-way mixed-design ANOVA; group effect: $F_{(1,18)} = 8.457$, $p = 0.0094$; dose effect: $F_{(3,54)} = 4.396$, $p = 0.0077$; interaction: $F_{(3,54)} = 8.509$, $p = 0.0001$; simple main effect of dose was significant for GFP^+ cells: $F_{(3,54)} = 12.10$, $p < 0.0001$; but not for GFP^- cells: $F_{(3,54)} = 0.809$, $p = 0.4942$). The responses of the GFP^+ cells at 0.05% and 0.1% PhAc were significantly higher than those of the GFP^- cells (simple main effect tests of group: $F_{(1, 72)} = 7.863$, $p = 0.0065$; and $F_{(1, 72)} = 25.09$, $p < 0.0001$, respectively). In addition to the slice electrophysiology, the data support the suggestion that IR84a/IR8a complex forms a functional receptor in response to exogenous ligands in the mammalian system.

In vivo activation of LC neurons stimulates NE release

To explore whether the IRNA technique can trigger *in vivo* noradrenergic activation, we performed an extracellular single-unit recording of LC NE neurons (Fig. 3*A*). NE cells in the LC were identified based on firing frequency and waveform as described previously (Takahashi et al., 2010). For the *in vivo* electrophysiology, we used the concentration of 1% of PhAc for pneumatic injection. The baseline firing rates (pre) of the Tg and non-Tg control mice were not significantly different from each other (1.13 ± 0.24 and 1.20 ± 0.21 Hz, respectively; unpaired two-tailed t test, $t_{(9)} = 0.205$, $p = 0.8425$). The injection of PhAc into the LC induced a robust increase of firing activity in the Tg mice, whereas LC neurons in the non-Tg controls were insensitive to PhAc injection (Fig. 3*B*, typical firing patterns). The firing rate of the Tg neurons was significantly increased to 3.73 ± 0.31 Hz (post) by the PhAc injection (Fig. 3*C*; $n = 6$; paired two-tailed t test, $t_{(5)} = 11.53$, $p < 0.0001$ vs pre), whereas the rate of the non-Tg mice did not alter by the injection (Fig. 3*C*; post: 1.22 ± 0.15 Hz; $n = 5$; paired two-tailed t test, $t_{(4)} = 0.300$, $p = 0.7788$ vs pre). When the effect of PhAc on the discharge of non-NE neurons around the LC was tested, these neurons were categorized into two groups showing low (0.1–4 Hz) and high (9–40 Hz) frequency of firing activity. The firing rate in each group was unaffected by PhAc injection (Fig. 3*D*; $n = 5$ or 7; paired two-tailed t test: $t_{(4)} = 0.460$, $p = 0.6696$ for low frequency; $t_{(6)} = 0.880$, $p = 0.4125$ for high frequency). The placement sites of the recording electrodes for *in vivo* electrophysiology are

shown in Figure 3*J*. These data indicated that ligand treatment indeed activates the *in vivo* firing of LC NE neurons harboring IR84a/IR8a.

To further assess ligand-induced noradrenergic activation, we measured NE release in the brain region innervated by the LC using a microdialysis procedure. We first tested NE release from the ACC (Fig. 3*E*), because the ACC is known to receive abundant innervations from the LC (Robertson et al., 2013; Chandler et al., 2014). When we performed LC microinjection with 0.1% PhAc (0.2 μl/site) in this microdialysis with the Tg mice, the extracellular NE level did not show a significant increase in the ACC (Fig. 3*F*; $n = 4$ for each group; two-way ANOVA; drug effect: $F_{(1,4)} = 1.508$, $p = 0.2868$; fraction effect: $F_{(6,24)} = 1.481$, $p = 0.2268$; interaction: $F_{(6,24)} = 1.747$, $p = 0.1531$). The placement sites of the injection needles into the LC, as well as those of the dialysis probes into the ACC are shown in Figure 3*K*. We then used higher concentrations of PhAc (0.4% and 0.6%) for LC microinjection. There was no significant difference in average tonic NE concentration (in picograms/sample) between the two kinds of mice during baseline fractions before the microinjection: Tg, 0.24 ± 0.07 ($n = 18$); non-Tg, 0.30 ± 0.08 ($n = 10$; unpaired two-tailed *t* test; $t_{(26)} = 0.518$, $p = 0.6091$). Injection of both 0.4% and 0.6% PhAc into the LC caused a rapid and transient increase in the extracellular NE level in the Tg mice (Fig. 3*G*; $n = 6$ for each group; two-way mixed-design ANOVA; drug effect: $F_{(2,15)} = 9.607$, $p = 0.0021$; fraction effect: $F_{(6,90)} = 6.446$, $p < 0.0001$; interaction: $F_{(12,90)} = 3.269$, $p = 0.0006$). The NE level at the 30 min fraction was significantly increased to ~157% and 233% of the baseline level for the 0.4% and 0.6% PhAc injections, respectively ($t_{(105)} = 2.215$; $p = 0.0289$ for 0.4% vs PBS, $p < 0.0001$ for 0.6% vs PBS, Holm–Bonferroni test), and the magnitude of the effect was dose dependent ($p = 0.0059$ for 0.6% vs 0.4%, Holm–Bonferroni test). The 0.6% PhAc injection induced a subsequent elevation in the NE level at a timing delayed after the first peak for 90 min fractions (Holm–Bonferroni test; vs PBS condition: $t_{(105)} = 3.892$, $p = 0.0005$; vs 0.4% PhAc condition: $t_{(105)} = 2.837$, $p = 0.0109$) and 120 min fractions (vs PBS condition: $t_{(105)} = 4.223$, $p < 0.0005$; vs 0.4% PhAc condition: $t_{(105)} = 3.564$, $p = 0.0011$), suggesting the presence of other complex mechanisms for IR-dependent neuronal activation in addition to the influx of monovalent cations. In the non-Tg mice, injection of 0.4% and 0.6% PhAc into the LC did not generate any significant changes in NE release (Fig. 3*G*; $n = 5$ for each group, two-way mixed-design ANOVA; drug effect: $F_{(2,12)} = 0.911$, $p = 0.4282$; fraction effect: $F_{(6,72)} = 0.474$, $p = 0.8255$; interaction: $F_{(12,72)} = 0.359$, $p = 0.9733$; Fig. 3*L*, placement sites of the injection needles into the LC as well as those of the dialysis probes into the ACC).

Next, we measured NE release from the BLA by using 0.4%/0.6% PhAc for LC microinjection (0.2 μl/site; Fig. 3*H*). There was no significant difference in average tonic NE concentration (picograms/sample) during baseline fractions before the microinjection between the Tg (1.14 ± 0.32, $n = 16$) and non-Tg (1.61 ± 0.18, $n = 15$) mice (unpaired two-tailed *t* test: $t_{(29)} = 1.229$, $p = 0.2288$). Injection of both 0.4% and 0.6% PhAc into the LC caused a rapid and long-lasting increase in the extracellular NE level in the Tg mice (Fig. 3*I*; $n = 5$ or 6 for each group, two-way mixed-design ANOVA; drug effect: $F_{(2,13)} = 5.160$, $p = 0.0224$; fraction effect: $F_{(6,78)} = 6.598$, $p < 0.0001$; interaction: $F_{(12,78)} = 2.318$, $p = 0.0137$). The NE level at the 30 min fraction was significantly increased to ~155% of the baseline level for 0.6% PhAc injection (Holm–Bonferroni test, $t_{(91)} = 3.216$, $p = 0.0054$ vs PBS). The 0.4% PhAc injection also increased the NE level at the 30 min fraction by ~136%, although this effect did not reach the statistical significance ($t_{(91)} = 1.871$, $p = 0.0645$ vs PBS). Both 0.4% and 0.6% PhAc induced a sustained elevation in the NE level following the fraction immediately after injection for 60 min ($t_{(91)} = 2.495$, $p = 0.0144$ for 0.6% vs PBS; $t_{(91)} = 3.420$, $p = 0.0028$ for 0.4% vs PBS), 90 min ($t_{(91)} = 2.478$, $p = 0.0150$ for 0.6% vs PBS; $t_{(91)} = 2.819$, $p = 0.0177$ for 0.4% vs PBS), and 120 min fractions ($t_{(91)} = 2.529$, $p = 0.0132$ for 0.6% vs PBS; $t_{(91)} = 3.055$, $p = 0.0089$ for 0.4% vs PBS). In the non-Tg mice, both 0.4% and 0.6% PhAc injections did not generate any significant changes in NE release (Fig. 3*I*; $n = 5$ for each group, two-way mixed-design ANOVA; drug effect: $F_{(2,12)} = 0.583$, $p = 0.5733$; fraction effect: $F_{(6,72)} = 1.743$, $p = 0.1234$; interaction: $F_{(12,72)} = 0.621$, $p = 0.8180$; Fig. 3*M*, sites of the injection needles into the LC and those of the dialysis probes into the BLA). These data demonstrated LC noradrenergic activation by the IRNA strategy, which resulted in the stimulated NE release in the nerve terminal regions innervated by the LC.

One week after the microdialysis experiments, mice were subjected to histologic analysis to validate the cytotoxicity of PhAc treatment to the mouse brain. Immunostaining for TH/NET indicated the normal localization of LC cells in the side injected with 0.4% and 0.6% PhAc (Fig. 4*A*). The ratio of the number of cells stained for TH or NET in the treated side relative to the intact side was calculated. There was no significant difference in the relative ratios of cell numbers among the treated groups (Fig. 4*B*; $n = 3$ for each group; one-way ANOVA; $F_{(2,6)} = 1.085$, $p = 0.3961$ for TH; and $F_{(2,6)} = 1.426$, $p = 0.3115$ for NET). Staining with cresyl violet showed no cell damage against LC neurons in the PhAc-treated side (Fig. 4*C*). Staining of cell death markers was performed, and IBO was used as a positive control to detect cell death signals. IBO (1 mg/ml) or PhAc (0.6%) was injected into the LC (0.2 μl/site) of the Tg mice, and LC sections were stained by TUNEL and immunohistochemistry for activated caspase-3. The number of these signals in the PhAc-treated side was significantly lower than that in the IBO-treated side (Fig. 4*D*), confirming the lack of cytotoxicity of PhAc treatment against LC cells expressing the receptors.

Ligand-induced LC activation results in enhanced memory retrieval

To address the role of LC NE neurons in memory retrieval, we conducted selective activation of these neurons using IRNA and investigated its impact on the retrieval process of conditioned taste aversion, in which mice learn an association between a taste stimulus and a visceral malaise-inducing stimulus (Yamamoto et al., 1994; Bermúdez-Rattoni, 2004). We used a taste reactivity test, which is a sensitive marker of taste aversion (Inui et al., 2013; Yasoshima and Shimura, 2017; Fig. 5*A*, behavioral procedure, *B*, experimental apparatus). In this paradigm, taste aversion memory was formed by repeated conditioning, in which the voluntary consumption of 0.5 M sucrose as a CS was followed by an intraperitoneal 0.15 M LiCl injection (2% of body weight) as a US. After the habituation period, mice received bilateral injections of PBS or PhAc solution into the LC (0.2 μl/site) 20 min before the intraoral infusion of the CS fluid. We used 0.4% and 0.6% PhAc, which induced a significant increase in NE level in the microdialysis experiment. The behavior of mice was recorded, and the latency to express the rejection responses (gaping, chin rubbing, forelimb flailing, paw wiping, and CS dropping) was measured during a 10 min test period. The latency to express the responses in the Tg mice differed significantly among the treatments into the LC (Fig. 5*C*; $n = 8$–9 for each group; $F_{(2,23)} = 7.214$, $p = 0.0037$), and the values for the 0.4% PhAc

injections (95.25 ± 14.25 s, $p = 0.0189$) and 0.6% PhAc injections (79.22 ± 12.39 s, $p = 0.0050$) showed a significant shortening compared with the PBS injection (196.78 ± 35.91 s). The latency for the PhAc injection into the non-Tg LC at the same concentrations (187.88 ± 42.62 s for 0.4% PhAc; 180.25 ± 35.88 s for 0.6% PhAc) demonstrated no significant differences compared with the PBS injection (189.09 ± 36.58 s; Fig. 5C; $n = 8$–11 for each group; $F_{(2,24)} = 0.0149$, $p = 0.9853$). The placement sites of injection needles into the LC for the taste reactivity test are shown in Figure 5F. These results suggest that PhAc-induced activation of LC NE neurons enhances the retrieval process of conditioned taste aversion.

During the recording of mouse behavior, we counted the number of rejection responses. The time course of the responses at a 10 s bin indicated that the responses were generated at earlier phases (<100 s) after the 0.4% or 0.6% PhAc injections, compared with the PBS injection in the Tg mice, whereas these changes were not seen in the non-Tg mice (Fig. 5D). These data support the shortening of latency for the initiation of rejection behaviors after 0.4% or 0.6% PhAc treatment in the Tg mice. In contrast, the total number of aversive responses during the 10 min test period was not significantly different among the three treatment groups in the Tg or non-Tg mice (Fig. 5E; one-way ANOVA; Tg mice: $n = 8$–9, $F_{(2,23)} = 0.969$, $p = 0.3945$; non-Tg mice: $n = 8$–11, $F_{(2,24)} = 0.033$, $p = 0.9677$), suggesting no apparent change in memory storage by the LC stimulation in our experimental condition. Therefore, the effect of ligand-induced LC activation on memory retrieval was evaluated by measuring the latency for rejection behaviors in the following analyses.

The reduction in the latency to express the rejection responses may be attributable to increased sensitivity to taste stimulus. To test this possibility, we examined whether the activation of LC NE neurons changes the sensitivity of taste by measuring the consumption of 0.5 M sucrose presented to unconditioned mice. Mice received the bilateral injection of PBS or PhAc solution (0.6%) into the LC (0.2 μl/site), and the fluid intake of 0.5 M sucrose was measured. In both the Tg and non-Tg mice, the intake was not significantly different between the PBS- or PhAc-injected groups (Fig. 6A; $n = 4$–7 for each group, unpaired two-tailed t test; Tg mice: $t_{(8)} = 0.061$, $p = 0.9531$; non-Tg mice: $t_{(11)} = 0.595$, $p = 0.5636$; Fig. 6E, placement sites of the injection needles for the taste sensitivity test of unconditioned mice). To further confirm that the activated LC NE neurons do not affect sensitivity to the taste stimulus, we checked the hedonic responses of unconditioned mice to 0.5 M sucrose using the taste reactivity test. The Tg mice were given a bilateral injection of PBS or 0.6% PhAc into their LC 20 min before the intraoral infusion of 0.5 M sucrose. Mouse behavior was recorded, and the latency to express the hedonic responses (tongue protrusion and lateral tongue protrusion) was measured. The latency for these responses did not significantly differ between the PBS-injected and PhAc-injected groups (28.83 ± 8.03 and 33.83 ± 8.33 s, respectively; Fig. 6B; $n = 6$ for each group; unpaired two-tailed t test; $t_{(10)} = 0.432$, $p = 0.6749$; Fig. 6F, sites of the injection needles for the taste reactivity test of unconditioned hedonic responses). These data exclude the possibility that the reduction in the latency by LC stimulation simply results from increased sensitivity to the taste stimulus.

It is also possible that the activation of LC NE neurons may promote a state of general arousal, resulting in enhancement of unconditioned responses to aversive events regardless of memory retrieval. To test this possibility, we examined whether the activation of LC NE neurons alters the rejection responses of mice to an unconditioned bitter tastant, quinine, using the reactivity test. The Tg mice received a bilateral injection of PBS or 0.6% PhAc into the LC 20 min before the intraoral infusion of 200 μM quinine solution, which induced substantial aversive responses. The latency for rejection responses was not significantly different between the PBS-injected and PhAc-injected groups (57.75 ± 13.26 and 54.25 ± 11.34 s, respectively; Fig. 6C; $n = 8$ for each group, unpaired two-tailed t test; $t_{(14)} = 0.201$, $p = 0.8439$; Fig. 6G, sites of the injection needles for the taste reactivity test of unconditioned aversive responses). These data indicate that the activation of LC NE neurons does not enhance the unconditioned response to aversive stimulus and exclude the possibility that the reduced latency by LC stimulation simply results from increased arousal level and potentiated general emotional responses to an innate gustatory stimulus.

In addition, the locomotor activity of the treated mice was monitored in the open field apparatus. Mice were habituated to the environment for 60 min and injected bilaterally with PBS and then with PhAc solution (0.6%) into the LC. Locomotor activity (60 min) was not significantly different among the Tg and non-Tg groups after PBS or PhAc injection (Fig. 6D; $n = 7$ for each group, two-way ANOVA; group effect: $F_{(1,12)} = 0.512$, $p = 0.4878$; time-block effect: $F_{(17,204)} = 60.47$, $p < 0.0001$; and interaction: $F_{(17,204)} = 0.480$, $p = 0.9599$; Fig. 6H, injection sites for the locomotion test). Locomotion of the Tg mice after PhAc injection was apparently normal, suggesting that the reduced latency of taste reactivity by LC stimulation cannot be explained by changes in general motor behavior by PhAc injection.

Based on this behavioral evidence, we conclude that the activation of LC NE neurons in response to the exogenous ligand promotes the retrieval process of aversive memory for events acquired through conditioning with a specific taste stimulus.

Neural pathway mediating enhanced memory retrieval through LC activation

The formation of conditioned taste aversion requires the function of the BLA in the amygdala (Yamamoto et al., 1994; Bermúdez-Rattoni, 2004), which receives innervation from LC NE neurons (Robertson et al., 2013; Chandler et al., 2014). To determine whether the LC–BLA noradrenergic pathway is involved in the enhancement of memory retrieval, we performed pharmacological blockade experiments for taste reactivity using PRAZ and PROP as α_1- and β-adrenergic receptor antagonists, respectively. First, to check doses of adrenergic receptor antagonists infused into the BLA that do not affect taste reactivity in wild-type mice, we tested the effect of bilateral intra-BLA treatment with PRAZ (0.1 or 0.5 μg/site) or PROP (0.4 or 2.0 μg/site) on the wild-type reactivity. The CS fluid was then intraorally infused, and the latency for reaction response initiation was measured. The latency to reject the CS differed significantly among the groups (Fig. 7A; $n = 7$–10; one-way ANOVA; $F_{(4,36)} = 4.830$, $p = 0.0032$), and the values for the groups treated with higher doses of PRAZ (340.75 ± 38.63 s) and PROP (334.57 ± 34.66 s) were significantly lengthened compared with the PBS-treated controls (156.1 ± 37.42 s; PRAZ, $p = 0.0138$; PROP, $p = 0.0252$). In contrast, the latency in the groups treated with lower doses of PRAZ (190.75 ± 39.12 s) or PROP (187.75 ± 47.88 s) did not show any significant differences compared with PBS treatment (PRAZ, $p = 0.9681$; PROP, $p = 0.9770$). The placement sites of the injection needles into the BLA for the taste reactivity test are shown in Figure 7D. Thus, intra-BLA infusion of lower doses of PRAZ and PROP does not influence the latency of taste reactivity in wild-type mice, whereas the data obtained from the use of higher doses

of the antagonists show the necessity of the BLA for the retrieval process of conditioned taste aversion.

Next, we tested whether enhanced memory retrieval by LC stimulation can be blocked by the intra-BLA treatment with lower doses of adrenergic receptor antagonists that do not affect taste reactivity in wild-type mice. The Tg and non-Tg mice were given the bilateral intra-BLA treatment of PRAZ (0.1 μg/site) or PROP (0.4 μg/site), which was then followed by the injection of PhAc solution (0.6%) into the LC (0.2 μl/site). The latency to reject the CS in the Tg mice significantly differed among the three groups (Fig. 7*B*; $n = 8$–9 for each group; one-way ANOVA; $F_{(2,23)} = 5.860$, $p = 0.0088$), and the values for the PRAZ-treated and PROP-treated groups (176.00 ± 26.81 and 199.11 ± 25.96 s, respectively) were significantly elevated compared with the PBS-treated controls (83.75 ± 19.63 s; PRAZ, $p = 0.0402$; PROP, $p = 0.0092$). By contrast, the latency in the non-Tg mice for the treatment of PRAZ (196.14 ± 47.75 s) or PROP (162.57 ± 37.33 s) displayed no significant differences compared with PBS treatment (186.43 ± 20.10 s; Fig. 7*B*; $n = 7$ for each group; $F_{(2,18)} = 0.220$, $p = 0.8050$; Fig. 7*E*, placement sites of the injection needles into the LC and BLA for the taste reactivity test). Therefore, the enhanced retrieval of conditioned taste aversion by LC noradrenergic activation is blocked by either α_1- or β-adrenergic antagonist treated into the BLA, suggesting that the retrieval process is mediated, in part, through α_1- and β-adrenergic receptor signaling via the LC–BLA pathway.

In addition, the locomotor activity of the treated mice was monitored in the open field apparatus. The Tg mice were habituated to the environment for 60 min and injected bilaterally with PBS, PRAZ (0.1 μg/site), or PROP (0.4 μg/site) into the BLA, and then with PhAc solution (0.6%) into the LC. Locomotor activity (60 min) was not significantly different among the treatment groups (Fig. 7*C*; $n = 4$ for each group; one-way ANOVA; $F_{(2,9)} = 0.0738$, $p = 0.9294$; Fig. 7*F*, sites of the injection needles into the LC and BLA for the locomotion test). The data suggest that the prolonged latency of taste reactivity by the treatment of adrenergic receptor antagonists into the BLA compared with the PBS injection cannot be attributed to changes in general motor behavior by drug treatment into the BLA.

Impact of pharmacological inhibition of LC neurons on memory retrieval

To ascertain the enhancing effect of LC noradrenergic activation on memory retrieval, we tested whether the inhibition of LC NE activity would suppress the retrieval process of conditioned taste aversion. Wild-type mice were given an infusion of CLO, which is an α_2-adrenergic receptor agonist that inhibits LC activity (Aghajanian and VanderMaelen, 1982; Washburn and Moises, 1989), with the lower (10 ng/site) and higher (25 ng/site) doses into the bilateral LC and subjected to the reactivity test. Latency to reject the CS differed significantly according to the treatments (Fig. 8*A*; $n = 7$–8 for each group; one-way ANOVA; $F_{(2,20)} = 17.19$, $p < 0.0001$), the value for the lower and higher doses of CLO (380.86 ± 20.13 and 292.50 ± 29.23 s, respectively) exhibited a significant lengthening compared with PBS injection (165.25 ± 26.14 s; $p < 0.0001$ for the lower dose; $p = 0.0055$ for the higher dose). The placement sites of the injection needles into the LC for the taste reactivity test are shown in Figure 8*D*. The inhibition of LC NE activity actually resulted in the suppression of the retrieval of taste associative memory, which is consistent with the facilitative role of these neurons in the memory retrieval process.

Another cohort of mice that received an intra-LC injection of CLO was subjected to the locomotion test. Wild-type mice were habituated to the environment for 60 min and injected bilaterally with the lower and higher doses of CLO into the LC. Locomotor activity (60 min) showed no significant difference among the treatment groups (Fig. 8*B*; $n = 6$ for each group one-way ANOVA; $F_{(2,15)} = 0.042$, $p = 0.959$). The placement sites of the injection needles into the LC for the locomotion test are indicated in Figure 8*E*. These data suggest that the lengthened latency of taste reactivity because of CLO treatment is not related to alterations in general motor behavior because of drug treatment into the LC.

To further validate adrenergic receptor function in the BLA during memory retrieval, we investigated whether the activation of adrenergic receptor subtypes in the BLA can restore suppressed memory retrieval by inhibition of LC activity. Wild-type mice received a bilateral intra-LC infusion of CLO (10 ng/site), and then bilateral intra-BLA treatment of α_1-adrenergic receptor agonist MET (0.5 μg/site) or β-adrenergic receptor agonist ISO (1.25 μg/site) before the taste reactivity test. The latency to reject the CS in the CLO-injected mice differed significantly according to treatment in the BLA (Fig. 8*C*; $n = 7$–8 for each group, one-way ANOVA; $F_{(2,20)} = 20.83$, $p < 0.0001$), and the values in MET and ISO treatment (169.00 ± 31.06 and 150.00 ± 21.45 s, respectively) showed a significant shortening compared with PBS treatment (462.00 ± 56.65 s, $p < 0.0001$ for the MET- and ISO-treated groups; Fig. 8*F*, injection sites into the LC and BLA for the taste reactivity test). The data indicate that α_1- or β-adrenergic receptor activation in the amygdala indeed recovered the impaired memory retrieval by LC inhibition, supporting the idea that the retrieval process of conditioned aversive memory is mediated at least partly through α_1-/β-adrenergic receptor signaling via the LC–BLA pathway.

Discussion

We have successfully developed IRNA as a novel chemogenetic approach to stimulate the activity of specific neuronal types and applied this technology to evaluate the behavioral role of LC NE neurons in memory retrieval. Here we discuss the advantages and limitations of IRNA compared with other chemogenetic systems, and consider the biological implications of our new insights into LC NE neuron function.

IRNA as a chemogenetic method for selective neuronal stimulation

An important consideration for any chemogenetic system is the minimization of activation of the chemogenetic receptor in the absence of external application of the cognate ligand. In this context, it is important to recognize that a low level of the IR84a/IR8a ligand PhAc (~0.3 μM) is present in rat brain and human CSF (Durden and Boulton, 1982; Sandler et al., 1982). However, in our *in vivo* electrophysiological experiments, the basal firing rates of LC NE neurons were similar between the Tg and non-Tg mice. Moreover, in the microdialysis assay, the tonic NE concentrations were also indistinguishable between the two kinds of mice. These data suggest that the IR84a/IR8a complex expressed in the Tg mice do not respond to any endogenous PhAc that might be present in the mouse brain. We used higher doses of PhAc for ligand treatments, and the effective doses were different among the experimental conditions. Compared with bath application of PhAc (0.1%, 7.3 mM) for slice electrophysiology, we required higher doses of the ligand (0.4%/0.6%) for *in vivo*

experiments, including the microdialysis and behavioral studies. Despite these higher doses of the ligand, our slice and *in vivo* electrophysiology experiments showed no significant differences in the firing properties in the non-Tg control mice between pre- and post-periods of PhAc treatment, and microdialysis and various behavioral experiments also indicated no significant differences in their values in the control mice between PBS and PhAc injections. Physiologic and behavioral changes were observed only in the Tg mice after PhAc injection. In addition, there were no cytotoxic effects on LC neurons in the Tg mice that received ligand injection.

In the present study, we focused on using IRNA to study the role of LC NE neurons in the retrieval process of taste associative memory. The Tg mouse strain generated here expresses the IR84a/IR8a transgene in other catecholaminergic cell groups, including dopaminergic neurons. Microinjection of the ligand into the brain regions containing these cell groups will cause the activation of the corresponding neurons. In addition, the use of other cell type-specific promoters with IRNA will enable us to stimulate the activity of target neurons of interest. Furthermore, future development of approaches for ligand delivery through the blood–brain barrier after systemic administration may be useful to target more conveniently a specific neuronal type in the brain.

The IR84a/IR8a complex forms an odorant-gated ionotropic cation channel that principally conducts monovalent cations (Na^+ and K^+), but it may also lead to a small amount of Ca^{2+} entry (Abuin et al., 2011; Ng et al., 2019). In the present study, microinjection of PhAc (0.4% and 0.6%) into the LC results in an increased NE release in the Tg brain, and, in particular, a higher dose of PhAc injection was followed by a sustained elevation of NE release in the ACC and BLA. It is possible that intracellular signaling cascades triggered by IR84a/IR8a-dependent Ca^{2+} influx contribute to the sustained elevation of NE release after high-dose PhAc injections. For instance, Ca^{2+}/calmodulin-dependent protein kinase II and protein kinase C mediate trafficking of glutamate receptors and long-term plasticity dependent on protein synthesis (MacDonald et al., 2001; Herring and Nicoll, 2016). Activation of protein kinase C also promotes TH gene expression and NE biosynthesis in catecholamine-producing cells (Vyas et al., 1990; Goc et al., 1992).

In our slice electrophysiology, ~30% of neurons caused depolarization block in response to 0.1% PhAc. Depolarization block is a generally observed phenomenon in excitatory ionic channels. However, this event was not observed in our *in vivo* electrophysiology. As mentioned above, the microdialysis experiment showed that PhAc treatment induced a sustained elevation of NE release in a dose-dependent manner. These data indicated that *in vivo* PhAc treatment caused the increased net activity of LC NE neurons in the Tg mice. In our preliminary experiments of *in vivo* electrophysiology, pneumatic injection of a high concentration of glutamate (>1 mM) frequently induces depolarization block. This suggests that the *in vivo* conditions of PhAc treatment in this study may have mild excitatory effects, which do not lead to depolarization block, on LC NE neurons expressing the IR84a/IR8a receptors.

Other chemogenetic systems have been based on designer receptors exclusively activated by designer drugs (DREADDs) to stimulate or inhibit the activity of specific neuronal types (Urban and Roth, 2015; Roth, 2016). For example, modified human muscarinic acetylcholine receptors, such as hM3Dq and hM4Di, are expressed in the target neuronal type and clozapine *N*-oxide (CNO), a ligand for the engineered receptors, is administered. However, CNO-induced cellular responsiveness requires endogenous G-proteins and relevant second-messenger cascades. In addition, CNO has multiple dose-dependent effects on wild-type animals through *in vivo* conversion to clozapine and *N*-desmethylclozapine, which act on several types of G-protein-coupled receptors (MacLaren et al., 2016) and engineered receptors (Gomez et al., 2017). By contrast, our IRNA technology depends on the expression of foreign ligand-gated excitatory IRs in specific neurons and does not require other signaling systems.

Another ion channel-based chemogenetic strategy has been reported, in which modified α7 nicotinic acetylcholine receptor ligand-binding domains are fused to an ion pore domain of serotonin receptor 3 (α7-5HT3) or glycine receptor (α7-GlyR; Magnus et al., 2011, 2019). The ligand varenicline shows a higher affinity to these chimeric receptors compared with endogenous acetylcholine. In the inhibitory α7-GlyR system, a single systemic injection of the ligand appears to cause sustained behavioral changes for 3–4 h, whereas the *in vivo* effects of the stimulatory α7-5HT3 system have not yet been reported. We have shown that IRNA is sufficient to produce behavioral effects, indicating the feasibility of this technology to validate both physiological and behavioral consequences of target neuron activation.

Finally, we note that the IR family of ionotropic olfactory receptors is large and functionally divergent (Croset et al., 2010; Rytz et al., 2013; van Giesen and Garrity, 2017); other members of the repertoire may be exploited in the future for applications of IRNA with different chemical ligands. The large range of candidate ion channels is valuable because IRNA technology requires coexpression of at least two subunits (Abuin et al., 2011; Rytz et al., 2013; van Giesen and Garrity, 2017), and it is possible that some will not show efficient expression or the expected ligand specificity when heterologously expressed in mammalian cells.

A key role for the LC NE system in the retrieval of taste associative memory

The present findings provide evidence for the key role of LC NE neurons in the retrieval process of conditioned taste aversion, showing that this role is mediated, in part, through α1- and β-adrenergic receptor subtypes via the LC–BLA pathway. A previous study with dopamine β-hydroxylase-deficient mice reports that NE transmission is involved in the retrieval of intermediate-term contextual fear and spatial memory requiring the hippocampus (Murchison et al., 2004), whereas pharmacological blockade of β-adrenergic receptors in the BLA does not influence the recall of conditioned odor aversion that depends on the association between an odor stimulus and a visceral malaise-inducing stimulus (Miranda et al., 2007). Conditioned odor aversion also requires amygdalar function (Ferry and Di Scala, 1997), and the acquisition of this aversion is disrupted by catecholamine depletion of amygdala (Fernandez-Ruiz et al., 1993) or the blockade of β-adrenergic receptor in the BLA (Miranda et al., 2007), suggesting a distinct mechanism for the maintenance or retrieval of conditioned aversive memory between sensory modalities.

A recent study reported that the BLA is required for the retrieval process of conditioned taste aversion (Inui et al., 2019). Therefore, the LC–BLA pathway may directly influence the activity of BLA neurons at the phase of memory retrieval of taste aversion. NE terminals are localized in both pyramidal neurons and GABAergic interneurons in the BLA (Li et al., 2001, 2002; Farb et al., 2010; Zhang et al., 2013). NE potentiates glutamate-mediated excitatory synaptic transmission through presynaptic mechanisms via β-adrenergic receptors in the amygdala (Huang et al., 1996; Ferry et al., 1997). NE facilitates GABA transmission

through presynaptic mechanisms via α_1-adrenergic receptors (Braga et al., 2004) and also excites some GABA interneurons directly via α_1-adrenoceptors (Kaneko et al., 2008). These potential synaptic mechanisms may underlie the facilitation of the retrieval process of taste aversion memory through the activation of the LC–BLA pathway. *In vivo* electrophysiological studies have reported that LC stimulation or NE iontophoresis inhibits spontaneous firing of the majority of BLA neurons and decreases the responsiveness of these neurons to cortical stimulation in normal conditions (Buffalari and Grace, 2007; Chen and Sara, 2007). However, in response to chronic stress exposure, NE increases spontaneous activity of BLA neurons and produces facilitation of responses evoked by cortical stimulation (Buffalari and Grace, 2009). These data suggest a dynamic shift in the NE response of amygdalar neurons dependent on the environmental conditions or emotional context.

Recent studies have reported that dopamine is released from LC terminals in the hippocampus and that LC-derived dopamine modulates memory formation (Kempadoo et al., 2016; Takeuchi et al., 2016). Similarly, dopamine may be released from LC terminals in the amygdala and is partly implicated in the retrieval process of amygdala-dependent memory; an important issue for future studies. In addition, LC NE neurons send their axon terminals to nuclei in the amygdala, including the BLA and central nucleus (CeN; Robertson et al., 2013; Chandler et al., 2014). Although some studies have reported the role of the CeN in taste aversion (Lamprecht et al., 1997; Bahar et al., 2003), whether the CeN is required for the learning process is controversial (Yamamoto et al., 1995). It remains unclear and to be explored whether LC projection to the CeN is involved in the retrieval process of the taste aversion task. The insular cortex is also required for the formation of taste aversion (Yamamoto et al., 1994; Bermúdez-Rattoni, 2004) and especially for long-term memory formation dependent on *de novo* protein synthesis and mitogen-activated protein kinase cascades (Rosenblum et al., 1993; Berman et al., 1998). These data suggest the engagement of the insular cortex to memory consolidation through interaction with the amygdala. This evidence suggests that LC noradrenergic neurons influence the interaction between the cortical and amygdalar regions to facilitate the recall of stored memory.

In conclusion, through the application of a novel chemogenetic method, the present study highlights that the LC NE system plays a facilitative role in the retrieval process of taste associative memory, in part, through adrenergic receptor signaling in the BLA. We focused on the study of LC NE function in taste aversion circuits, and we need to investigate whether the finding on the role of these neurons in memory recall is applicable for other types of memory paradigms. Dysfunction of the central NE system is implicated in the pathologic states of neuropsychiatric diseases, such as Korsakoff's syndrome with anterograde and retrograde amnesia, post-traumatic amnesia, and post-traumatic stress disorder (Chamberlain and Robbins, 2013; Hendrickson and Raskind, 2016). Adrenergic receptor subtypes are potential therapeutic targets for post-traumatic stress disorder (Strawn and Geracioti, 2008). A detailed analysis of the neural substrate that mediates memory retrieval dependent on the LC–amygdalar NE system may provide insight leading to a deeper understanding of the mechanisms underlying the pathogenesis of these neuropsychiatric diseases.

References

Abuin L, Bargeton B, Ulbrich MH, Isacoff EY, Kellenberger S, Benton R (2011) Functional architecture of olfactory ionotropic glutamate receptors. Neuron 69:44–60.

Aghajanian GK, VanderMaelen CP (1982) alpha 2-adrenoceptor-mediated hyperpolarization of locus coeruleus neurons: intracellular studies in vivo. Science 215:1394–1396.

American Psychiatric Association (2013) Diagnostic and statistical manual of mental disorders, Ed 5. Washington, DC: American Psychiatric Association.

Bahar A, Samuel A, Hazvi S, Dudai Y (2003) The amygdalar circuit that acquires taste aversion memory differs from the circuit that extinguishes it. Eur J Neurosci 17:1527–1530.

Benton R, Vannice KS, Gomez-Diaz C, Vosshall LB (2009) Variant ionotropic glutamate receptors as chemosensory receptors in Drosophila. Cell 136:149–162.

Berman DE, Hazvi S, Rosenblum K, Seger R, Dudai Y (1998) Specific and differential activation of mitogen-activated protein kinase cascades by unfamiliar taste in the insular cortex of the behaving rat. J Neurosci 18:10037–10044.

Bermúdez-Rattoni F (2004) Molecular mechanisms of taste-recognition memory. Nat Rev Neurosci 5:209–217.

Braga MF, Aroniadou-Anderjaska V, Manion ST, Hough CJ, Li H (2004) Stress impairs α_{1A} adrenoceptor-mediated noradrenergic facilitation of GABAergic transmission in the basolateral amygdala. Neuropsychopharmacol 29:45–58.

Buffalari DM, Grace AA (2007) Noradrenergic modulation of basolateral amygdala neuronal activity: opposing influences of α-2 and β receptor activation. J Neurosci 27:12358–12366.

Buffalari DM, Grace AA (2009) Chronic cold stress increases excitatory effects of norepinephrine on spontaneous and evoked activity of basolateral amygdala neurons. Int J Neuropsychopharmacol 12:95–107.

Bush DE, Caparosa EM, Gekker A, Ledoux J (2010) Beta-adrenergic receptors in the lateral nucleus of the amygdala contribute to the acquisition but not the consolidation of auditory fear conditioning. Front Behavi Neurosci 4:154.

Chamberlain SR, Robbins TW (2013) Noradrenergic modulation of cognition: therapeutic implications. J Psychopharmacol (Oxford) 27:694–718.

Chandler DJ, Gao WJ, Waterhouse BD (2014) Heterogeneous organization of the locus coeruleus projections to prefrontal and motor cortices. Proc Natl Acad Sci U S A 111:6816–6821.

Chen FJ, Sara SJ (2007) Locus coeruleus activation by foot shock or electrical stimulation inhibits amygdala neurons. Neurosci 144:472–481.

Croset V, Rytz R, Cummins SF, Budd A, Brawand D, Kaessmann H, Gibson TJ, Benton R (2010) Ancient protostome origin of chemosensory ionotropic glutamate receptors and the evolution of insect taste and olfaction. PLoS Genet 6:e1001064.

Devauges V, Sara SJ (1991) Memory retrieval enhancement by locus coeruleus stimulation: evidence for mediation by β-receptors. Behav Brain Res 43:93–97.

Durden DA, Boulton AA (1982) Identification and distribution of phenylacetic acid in the brain of the rat. J Neurochem 38:1532–1536.

Farb CR, Chang W, LeDoux JE (2010) Ultrastructural characterization of noradrenergic axons and beta-adrenergic receptors in the lateral nucleus of the amygdala. Front Behav Neurosci 4:162.

Fernandez-Ruiz J, Miranda MI, Bermúdez-Rattoni F, Drucker-Colín R (1993) Effects of catecholaminergic depletion of the amygdala and insular cortex on the potentiation of odor by taste aversions. Behav Neural Biol 60:189–191.

Ferry B, Di Scala G (1997) Bicuculline administration into basolateral amygdala facilitates trace conditioning of odor aversion in the rat. Neurobiol Learn Mem 67:80–83.

Ferry B, Magistretti PJ, Pralong E (1997) Noradrenaline modulates glutamate-mediated neurotransmission in the rat basolateral amygdala *in vitro*. Eur J Neurosci 9:1356–1364.

Ferry B, Parrot S, Marien M, Lazarus C, Cassel JC, McGaugh JL (2015) Noradrenergic influences in the basolateral amygdala on inhibitory avoidance memory are mediated by an action on α2-adrenoceptors. Psychoneuroendocrinol 51:68–79.

Franklin KBJ, Paxinos G (2008) The mouse brain in stereotaxic coordinates, Ed 3. Boston: Elsevier/Academic.

Gelinas JN, Nguyen PV (2005) β-Adrenergic receptor activation facilitates induction of a protein synthesis-dependent late phase of long-term potentiation. J Neurosci 25:3294–3303.

Goc A, Norman SA, Puchacz E, Stachowiak EK, Lukas RJ, Stachowiak MK (1992) A 5'-flanking region of the bovine tyrosine hydroxylase gene is involved in cell-specific expression, activation of gene transcription by

phorbol ester, and transactivation by c-Fos and c-Jun. Mol Cell Neurosci 3:383–394.

Gomez JL, Bonaventura J, Lesniak W, Mathews WB, Sysa-Shah P, Rodriguez LA, Ellis RJ, Richie CT, Harvey BK, Dannals RF, Pomper MG, Bonci A, Michaelides M (2017) Chemogenetics revealed: DREADD occupancy and activation via converted clozapine. Science 357:503–507.

Grosjean Y, Rytz R, Farine JP, Abuin L, Cortot J, Jefferis GSXE, Benton R (2011) An olfactory receptor for food-derived odours promotes male courtship in Drosophila. Nature 478:236–240.

Guzmán-Ramos K, Osorio-Gómez D, Moreno-Castilla P, Bermúdez-Rattoni F (2012) Post-acquisition release of glutamate and norepinephrine in the amygdala is involved in taste-aversion memory consolidation. Learn Mem 19:231–238.

Hendrickson RC, Raskind MA (2016) Noradrenergic dysregulation in the pathophysiology of PTSD. Exp Neurol 284:181–195.

Herring BE, Nicoll RA (2016) Long-term potentiation: from CaMKII to AMPA receptor trafficking. Annu Rev Physiol 78:351–365.

Huang CC, Hsu KS, Gean PW (1996) Isoproterenol potentiates synaptic transmission primarily by enhancing presynaptic calcium influx via P- and/or Q-type calcium channels in the rat amygdala. J Neurosci 16:1026–1033.

Huang YY, Kandel ER (1996) Modulation of both the early and the late phase of mossy fiber LTP by the activation of β-adrenergic receptors. Neuron 16:611–617.

Huang YY, Kandel ER (2007) Low-frequency stimulation induces a pathway-specific late phase of LTP in the amygdala that is mediated by PKA and dependent on protein synthesis. Learn Mem 14:497–503.

Huang YY, Martin KC, Kandel ER (2000) Both protein kinase A and mitogen-activated protein kinase are required in the amygdala for the macromolecular synthesis-dependent late phase of long-term potentiation. J Neurosci 20:6317–6325.

Inui T, Inui-Yamamoto C, Yoshioka Y, Ohzawa I, Shimura T (2013) Activation of efferents from the basolateral amygdala during the retrieval of conditioned taste aversion. Neurobiol Learn Mem 106:210–220.

Inui T, Sugishita T, Inui-Yamamoto C, Yasoshima Y, Shimura T (2019) The basolateral nucleus of the amygdala executes the parallel processes of avoidance and palatability in the retrieval of conditioned taste aversion in male rats. eNeuro 6:ENEURO.0004-19.2019.

Johansen JP, Diaz-Mataix L, Hamanaka H, Ozawa T, Ycu E, Koivumaa J, Kumar A, Hou M, Deisseroth K, Boyden ES (2014) Hebbian and neuromodulatory mechanisms interact to trigger associative memory formation. Proc Natl Acad Sci U S A 111:E5584–E5592.

Kaneko K, Tamamaki N, Owada H, Kakizaki T, Kume N, Totsuka M, Yamamoto T, Yawo H, Yagi T, Obata K, Yanagawa Y (2008) Noradrenergic excitation of a subpopulation of GABAergic cells in the basolateral amygdala via both activation of nonselective cationic conductance and suppression of resting K^+ conductance: a study using glutamate decarboxylase 67-green fluorescent protein knock-in mice. Neurosci 157:781–797.

Kato S, Inoue K, Kobayashi K, Yasoshima Y, Miyachi S, Inoue S, Hanawa H, Shimada T, Takada M, Kobayashi K (2007) Efficient gene transfer via retrograde transport in rodent and primate brains using a human immunodeficiency virus type 1-based vector pseudotyped with rabies virus glycoprotein. Hum Gene Ther 18:1141–1152.

Kempadoo KA, Mosharov EV, Choi SJ, Sulzer D, Kandel ER (2016) Dopamine release from the locus coeruleus to the dorsal hippocampus promotes spatial learning and memory. Proc Natl Acad Sci U S A 113:14835–14840.

Klein SB, Nichols S (2012) Memory and the sense of personal identity. Mind 483:677–702.

Kobayashi K, Noda Y, Matsushita N, Nishii K, Sawada H, Nagatsu T, Nakahara D, Fukabori R, Yasoshima Y, Yamamoto T, Miura M, Kano M, Mamiya T, Miyamoto Y, Nabeshima T (2000) Modest neuropsychological deficits caused by reduced noradrenaline metabolism in mice heterozygous for a mutated tyrosine hydroxylase gene. J Neurosci 20:2418–2426.

Kopelman MD (1992) The psychopharmacology of human memory disorders. In: Clinical management of memory problems (Wilson B, Moffat N, eds), pp 189–215. Boston: Springer.

LaLumiere RT, Buen TV, McGaugh JL (2003) Post-training intra-basolateral amygdala infusions of norepinephrine enhance consolidation of memory for contextual fear conditioning. J Neurosci 23:6754–6758.

Lamprecht R, Hazvi S, Dudai Y (1997) cAMP response element-binding protein in the amygdala is required for long- but not short-term conditioned taste aversion memory. J Neurosci 17:8443–8450.

Li R, Nishijo H, Wang Q, Uwano T, Tamura R, Ohtani O, Ono T (2001) Light and electron microscopic study of cholinergic and noradrenergic elements in the basolateral nucleus of the rat amygdala: evidence for interactions between the two systems. J Comp Neurol 439:411–425.

Li R, Nishijo H, Ono T, Ohtani Y, Ohtani O (2002) Synapses on GABAergic neurons in the basolateral nucleus of the rat amygdala: double-labeling immunoelectron microscopy. Synapse 43:42–50.

MacDonald JF, Kotecha SA, Lu VVY, Jackson MF (2001) Convergence of PKC-dependent kinase signal cascades on NMDA receptors. Curr Drug Targets 2:299–312.

MacLaren DAA, Browne RW, Shaw JK, Radhakrishnan SK, Khare P, España RA, Clark SD (2016) Clozapine N-oxide administration produces behavioral effects in Long–Evans rats: implications for designing DREADD experiments. eNeuro 3:ENEURO.0219-16.2016.

Magnus CJ, Lee PH, Atasoy D, Su HH, Looger LL, Sternson SM (2011) Chemical and genetic engineering of selective ion-channel–ligand interactions. Science 333:1292–1296.

Magnus CJ, Lee PH, Bonaventura J, Zemla R, Gomez JL, Ramirez MH, Hu X, Galvan A, Basu J, Michaelides M, Strernson SM (2019) Ultrapotent chemogenetics for research and potential clinical applications. Science 364:eaav5282.

Matsushita N, Okada H, Yasoshima Y, Takahashi K, Kiuchi K, Kobayashi K (2002) Dynamics of tyrosine hydroxylase promoter activity during midbrain dopaminergic neuron development. J Neurochem 82:295–304.

Miranda MA, Ferry B, Ferreira G (2007) Basolateral amygdala noradrenergic activity is involved in the acquisition of conditioned odor aversion in the rat. Neurobiol Learn Mem 88:260–263.

Murchison CF, Zhang XY, Zhang WP, Ouyang M, Lee A, Thomas SA (2004) A distinct role for norepinephrine in memory retrieval. Cell 117:131–143.

Ng R, Salem SS, Wu ST, Wu M, Lin HH, Shepherd AK, Joiner WJ, Wang JW, Su CY (2019) Amplification of Drosophila olfactory responses by a DEG/ENaC channel. Neuron 104:947–959.

O'Dell TJ, Connor SA, Gelinas JN, Nguyen PV (2010) Viagra for your synapses: enhancement of hippocampal long-term potentiation by activation of beta-adrenergic receptors. Cell Signal 22:728–736.

Osanai M, Saegusa H, Kazuno A, Nagayama S, Hu Q, Zong S, Murakoshi T, Tanabe T (2006) Altered cerebellar function in mice lacking $Ca_V2.3$ Ca^{2+} channel. Biochem Biophys Res Commun 344:920–925.

Robertson SD, Plummer NW, de Marchena J, Jensen P (2013) Developmental origins of central norepinephrine. Nat Neurosci 16:1016–1023.

Rosenblum K, Meiri N, Dudai Y (1993) Taste memory: the role of protein synthesis in gustatory cortex. Behav Neural Biol 59:49–56.

Roth BL (2016) DREADDs for neuroscientists. Neuron 89:683–694.

Rytz R, Croset V, Benton R (2013) Ionotropic receptors (IRs): chemosensory ionotropic glutamate receptors in Drosophila and beyond. Insect Biochemi Mol Biol 43:888–897.

Sandler M, Ruthven CR, Goodwin BL, Lees A, Stern GM (1982) Phenylacetic acid in human body fluids: high correlation between plasma and cerebrospinal fluid concentration values. J Neurol Neurosurg Psychiatry 45:366–368.

Sara SJ, Devauges V (1988) Priming stimulation of locus coeruleus facilitates memory retrieval in the rat. Brain Res 438:299–303.

Sawamoto K, Nakao N, Kobayashi K, Matsushita N, Takahashi H, Kakishita K, Yamamoto A, Yoshizaki T, Terashima T, Murakami F, Itakura T, Okano H (2001) Visualization, direct isolation, and transplantation of midbrain dopaminergic neurons. Proc Natl Acad Sci U S A 98:6423–6428.

Strawn JR, Geracioti TD Jr (2008) Noradrenergic dysfunction and the psychopharmacology of posttraumatic stress disorder. Depress Anxiety 25:260–271.

Takahashi K, Kayama Y, Lin JS, Sakai K (2010) Locus coeruleus neuronal activity during the sleep-waking cycle in mice. Neuroscience 169:1115–1126.

Takeuchi T, Duszkiewicz AJ, Sonneborn A, Spooner PA, Yamasaki M, Watanabe M, Smith CC, Fernández G, Deisseroth K, Greene RW, Morris RGM (2016) Locus coeruleus and dopaminergic consolidation of everyday memory. Nature 537:357–362.

Tarradas A, Selga E, Beltran-Alvarez P, Pérez-Serra A, Riuró H, Picó F, Iglesias A, Campuzano O, Castro-Urda V, Fernández-Lozano I, Pérez GJ, Scornik FS, Brugada R and (2013) A novel missense mutation, I890T, in the pore region of cardiac sodium channel causes Brugada syndrome. PLoS One 8:e53220.

Urban DJ, Roth BL (2015) DREADDs (designer receptors exclusively activated by designer drugs): chemogenetic tools with therapeutic utility. Annu Rev Pharmacol Toxicol 55:399–417.

van den Pol AN, Ghosh PK, Liu R-j, Li Y, Aghajanian GK, Gao X-B (2002) Hypocretin (orexin) enhances neuron activity and cell synchrony in developing mouse GFP-expressing locus coeruleus. J Physiol 541:169–185.

van Giesen L, Garrity PA (2017) More than meets the IR: the expanding roles of variant ionotropic glutamate receptors in sensing odor, taste, temperature and moisture. F1000Res 6:1753.

Villain H, Benkahoul A, Drougard A, Lafragette M, Muzotte E, Pech S, Bui E, Brunet A, Birmes P, Roullet P (2016) Effects of propranolol, a β-noradrenergic antagonist, on memory consolidation and reconsolidation in mice. Front Behav Neurosci 10:49.

Vyas S, Faucon Biguet N, Mallet J (1990) Transcriptional and post-transcriptional regulation of tyrosine hydroxylase gene by protein kinase C. EMBO J 9:3707–3712.

Warrington EK, Weiskrantz L (1970) Amnesic syndrome: consolidation or retrieval? Nature 228:628–630.

Washburn M, Moises HC (1989) Electrophysiological correlates of presynaptic alpha 2-receptor-mediated inhibition of norepinephrine release at locus coeruleus synapses in dentate gyrus. J Neurosci 9:2131–2140.

Yamamoto T, Shimura T, Sako N, Yasoshima Y, Sakai N (1994) Neural substrates for conditioned taste aversion in the rat. Behav Brain Res 65:123–137.

Yamamoto T, Fujimoto Y, Shimura T, Sakai N (1995) Conditioned taste aversion in rats with excitotoxic brain lesions. Neurosci Res 22:31–49.

Yasoshima Y, Shimura T (2017) Midazolam impairs the retrieval of conditioned taste aversion via opioidergic transmission in mice. Neurosci Lett 636:64–69.

Zhang J, Muller JF, McDonald AJ (2013) Noradrenergic innervation of pyramidal cells in the rat basolateral amygdala. Neuroscience 228:395–408.

Zhang X, Cui N, Wu Z, Su J, Tadepalli JS, Sekizar S, Jiang C (2010) Intrinsic membrane properties of locus coeruleus neurons in *Mecp2*-null mice. Am J Physiol Cell Physiol 298:C635–C646.

Zhou J, Luo Y, Zhang J-T, Li M-X, Wang C-M, Guan X-L, Wu P-F, Hu Z-L, Jin Y, Ni L, Wang F, Chen J-G (2015) Propranolol decreases retention of fear memory by modulating the stability of surface glutamate receptor GluA1 subunits in the lateral amygdala. Br J Pharmacol 172:5068–5082.